



Mauritius Research and Innovation Council
INNOVATION FOR TECHNOLOGY

**ASSESSING THE EFFICACY
OF SOLAR CHIMNEYS IN
MAURITIUS THROUGH
DYNAMIC SIMULATIONS
AND IN-SITU
MEASUREMENTS**

Final Report

June 2021

Mauritius Research and Innovation Council

Address:
Level 6, Ebene Heights
34, Cybercity
Ebene

Telephone: (230) 465 1235
Fax: (230) 465 1239
e-mail: contact@mric.mu
Website: www.mric.mu

This report is based on work supported by the Mauritius Research Council under award number MRC/RUN-1734. Any opinions, findings, recommendations and conclusions expressed herein are the author's and do not necessarily reflect those of the Council.

MAURITIUS RESEARCH & INNOVATION
COUNCIL REPORT

**Assessing the efficacy of solar chimneys in Mauritius through
dynamic simulations and in-situ measurements**

Principal Investigator

Mahendra Gooroochurn (FoE)

Project collaborators

Roddy Lollchund (FoS)

Prof S D D V Rughooputh (FoS)

Heman Shamachurn (FoE)

Reshma Rughooputh (FoE)

UNIVERSITY OF MAURITIUS

January 2021

Table of Contents

1. Introduction.....	1
2. Literature Review	2
2.3 Vertical roof wall.....	11
2.4 Inclined roof chimney.....	11
3. Experimental Set-up of a solar chimney.....	16
3.1 Instrument used in assessing important parameter in solar chimney.....	17
4. Simulation Results and Discussion	19
5. Experimental Results and Discussion	32
6. Discussion and Conclusion	38

1. Introduction

Solar chimney is also commonly known as thermal chimney and it has been shown used in various contexts to improve the ventilation in modern buildings by mainly the process of convection. The working mechanism of solar chimney is based on the draft created when air is heated, which can be achieved using either transparent glazed areas and/or dark surfaces which tend to absorb solar radiation. Solar radiation is incident on a solar collector which can be placed on various positions depending on the configuration of the building. Consequently, the temperature near the region of the collector rises and creates a convection current of air. Passive solar chimney system can be considered as part of building design to reduce the heating and cooling loads, and hence improve energy efficiency.

Solar chimney has potential benefits in terms of operation cost, energy requirement and low carbon dioxide emission and has received interest across several climate zones countries. The daily energy consumption of an air-conditioner can be reduced at a rate of 10-20% by use of solar chimney as shown in a study in Thailand. Miyazaki et al. (2006) studied the performance of a solar chimney in an office building in Tokyo. They concluded that the daily energy required for ventilation decreased by 90% in January and February. The reduction was about 50% over the year. The design of a solar chimney with optimized performance at a low cost is the main challenge but numerous parameters come into play and plays an influential role in the design.

Given the previous interest in solar chimney in the Mauritian context and challenges faced in integrating it into the local concrete architecture, this study focused on the previous works carried out in the field of solar chimney, while proposing a design which will appeal to the local construction industry, not incur significant changes in structural needs of buildings and realisable using local workmanship. The review focused on the two main types of solar chimney namely vertical wall chimney and inclined roof solar chimney to understand the design variables and results obtained therewith. For both types, a review was done based on the mathematical models used, the influence factors involved and the previous works performed in terms of CFD, experimental or numerical analysis as described in the next section.

2. Literature Review

The two main types of solar chimneys presented in literature are the vertical solar chimney and roof solar chimney configurations. Figure 1 depicts these two solar chimney configurations and Table 1 highlights the main pros and cons of each one as described by Harris et al. (2007)

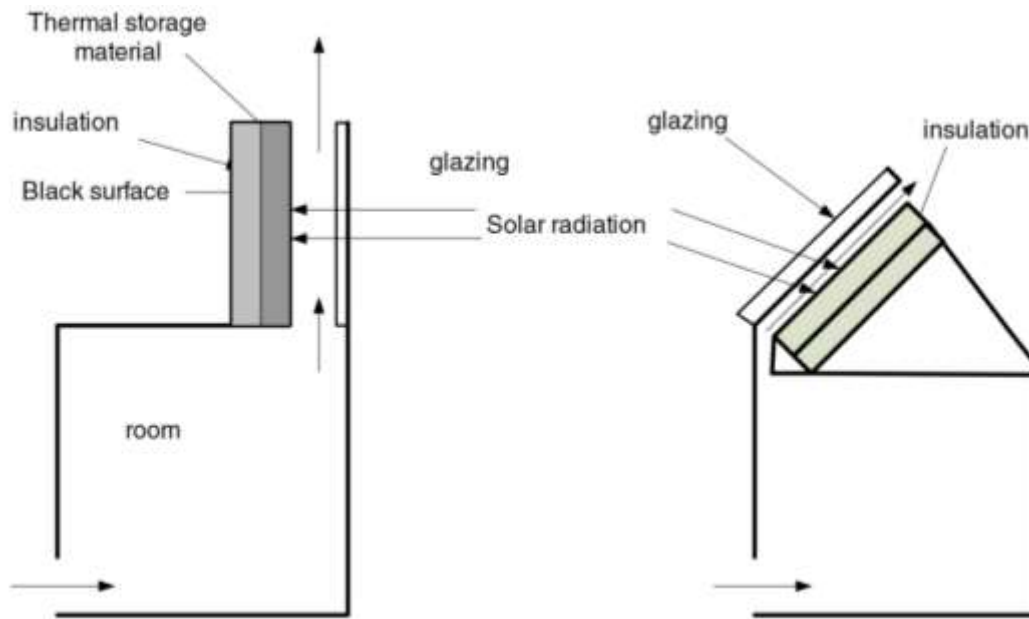


Figure 1: Solar chimney and building ventilation (Harris et al. (2007))

Table 1: Comparison between vertical and roof solar chimney (Harris et al. (2007))

	Vertical solar chimney	Roof solar chimney
Advantages	<ol style="list-style-type: none"> 1. The external glass gain sun radiation, hence solar collector not required 2. The air flow in chimney go up directly without bends 3. Easier to control inlet and outlet for different climatic conditions 4. Stack height is not restricted by roof height 	<ol style="list-style-type: none"> 1. Very large collector areas easily achieved 2. Maybe more aesthetically pleasing than a tower 3. Likely to be cheaper than tower designs 4. Easier to retrofit

Disadvantages

1. Insulation is needed to prevent direct heat transfer between chimney and interior room
2. Barrier are strictly prevented because the solar gained wall is lower than the roof solar collector

1. Stack height is restricted by roof height
2. Additional bends create greater pressure losses

2.1 Vertical roof chimney

This section describes the vertical roof chimney configuration in terms of underlying mathematical models, influencing factors and previous results.

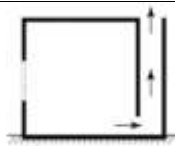
System description

A solar chimney is essentially divided into two parts, (1) the solar air heater (collector) and (2) the chimney. The system performance is dependent on the amount of solar heat gain, which in turn affects the ventilation rate achievable under a given solar yield condition. The critical design parameters are the height, cross-sectional area and the difference in temperature at the inlet and outlet of the system. Air in the solar collector gets heated during the day when exposed to solar radiation, expands and rises, in turn causing a negative draft which can be used to draw air from the interior space.

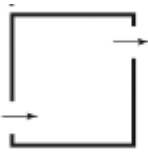
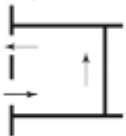
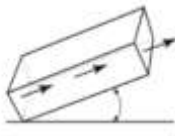
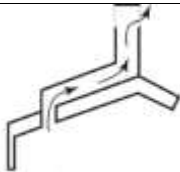
(a) Mathematical models

The various solar chimney designs reviewed by Shi et al. (2018) are tabulated below along with the appropriate modelling equations.

Table 2: Typical mathematical models for vertical solar chimneys (Shi et al (2018))

Typical Mathematical Models for Vertical Solar Chimney			
Reference	Year	Schematic	Equation
Shi and Zhang	2016		$C_{room} = [hHA_{hot}(T_{wall} - T_o)]^{1/3}$
Ryan and Burek	2010		$V \propto q^{0.459}$ $V \propto d^{0.756}$ $V \propto H^{0.600}$

Dimoudi	2009		$V = 23.37 A_{in} A_{out} \sqrt{\frac{gH(T_c - T_o)}{(K_{in} A_{out}^2 + K_{out} A_{in}^2) T_o T_c}}$
Sankonidou et al.	2008		$V = \sin\theta A_{out} \sqrt{\frac{2gH(e_o - e_c)}{(f \frac{H}{d} + K_{in} + K_{out}) e_c}}$
Sankonidou et al.	2008		$V = C_d \sin\theta \frac{e_c}{e_o} A_o \sqrt{\frac{gH(T_c - T_o)}{T_o}}$
Shen et al.	2007		$V = C_d A \sqrt{\frac{gH(T_{out} - T_{in})}{T_{out} + T_{in}}}$
Burek and Habeb	2007		$V \propto Q^{0.572}$ $V \propto d^{0.712}$
Ryan et al.	2005		$V \propto q^{0.452}$ $V \propto d^{0.652}$ $V \propto H^{0.539}$
Halldorsson et al.	2002		$V = A \left[\frac{gqwsin\theta H^2}{AeC_p T_o [f \frac{H}{d} + K_{in} (\frac{A}{A_{in}})^2 + k_{out} (\frac{A}{A_{out}})^2]} \right]^{1/3}$
Sandberg and Moshfegh	1998		$V = A \left[\frac{gqH^2 sin\theta}{(e_o C_p T_o d [2f \frac{H}{d} + K_{in} + 1])} \right]^{1/3}$
Gan	1998		$V = 143.4 w^{0.6582}$ $V = 4.5725 q^{0.4015}$ $V = 17.84\sqrt{H - 2.28} + 24.86$

Andersen	1995		$V = C_d A_{in} \sqrt{\frac{2gH(T_c - T_o)}{T_c}}$ $V = 0.037 (QH)^{1/3} (C_d A_{in})^{2/3}$
Awbi and Gan	1992		$V = C_d A \sqrt{\frac{4gH(T_c - T_o)}{T_c}}$
BS 5925	1991		$V = C_d \left[\frac{A_{in} A_{out}}{A_{in}^2 + A_{out}^2} \right] \sqrt{\frac{2gH(T_c - T_o)}{T_o}}$
Shi et al.	2016		$V = w(\sin \theta)^{1/3} q^{1/2} d^{0.7} H^{2/3}$
Afonso and Oliveira	2000		$V = \frac{A_{out} \sqrt{2\alpha g(T_c - T_o)H}}{\sqrt{K_{in} \frac{A_{out}^2}{A_{in}} + K_{out} + f \left(\frac{H}{d} \right)}}$
Bansal et al.	1993		$V = C_d A_{out} \sqrt{\frac{2(T_c - T_o)gH \sin \theta}{T_o(1 + A_r^2)}}$

Abbreviations			
A	area, m ²	Q	heat input
C	coefficient	W	Slope
Cp	specific heat capacity, J/kg°C	T	temperature, °C
d	air gap thickness, m	V	volumetric flow rate, m ³ /s
f	wall friction coefficient	w	cavity width, m
g	gravitational acceleration, m/s ²	α	thermal expansion coefficient, 1/°C
H	cavity height, m	θ	inclination angle from the horizontal, °
h	heat transfer coefficient, W/m ² °C	θ'	calculated inclination angle
k	pressure loss coefficient	ρ	density, kg/ m ³
q	heat input intensity, W/m ²		

Subscripts			
o	ambient conditions	out	outlet
c	cavity	r	ratio between outlet and inlet
d	discharge	room	room configuration
hot	hot cavity	wall	cavity wall.
in	inlet		

(b) Influencing factors

i. Height

The height for wall solar chimney refers to the vertical height of the chimney cavity. It is generally the case that a higher height can result in a better performance due to the greater pressure difference caused by the high chimney cavity, and the increased heat gain. Gan (1998) observed an increase of heat gains by three quarters after increasing the wall height by a quarter. Many studies have confirmed the same result. The ventilation flow was found to be increase proportionately when the chimney height is doubled.

AboulNaga and Abdrabboh (2000) analysed theoretically a chimney with heights within 1.95–3.45 m, and obtained the maximum air flow rate of 2.3 m³/s happens at a chimney height of 3.45 m. A numerical study by Lee and Strand (2009) stated that air flow rate increases by about 73% when the wall height rises from 3.5 m to 9.5 m with a 0.3 m cavity gap. Al-Kayiem et al. (2014) obtained numerically that the maximum air velocity rises from 3.47 m/s to 4.5 m/s when height rises from 5 m to 15 m. Therefore, Du et al. (2011) suggested to select the longest vertical length as possible within the restriction of building codes to achieve the best performance.

Waraporn Rattanongphisat et al. (2017) constructed and investigated experimentally, under real climate conditions, the performance of a square steel solar chimney used for building ventilation application. Air temperature and air flow results permit to conclude that the investigated solar chimney can be used for building ventilation even with a low height chimney.

ii. Height to gap ratio

Height/gap ratio usually refers to the ratio between cavity height and gap. The effects of height/gap ratio on the performance are then determined by the combination of these two parameters. Zamora and Kaiser (2009) studied, through numerical investigation, the laminar and turbulent flows induced by natural convection in channels, with side wall solar chimney configuration, for a wide range of Rayleigh number and several values of the relative wall-to-wall spacing. The opening from the room to the chimney gap is located at the bottom. They recommended an optimum gap-to-height ratio in correlation format, as function of Raynumber ranging from 105 to 1012.

Several studies have focused on obtaining the optimum height/gap ratio. An optimum ratio of 10 was obtained from both numerical modelling and experiments. Wang et al. (2015) indicated based on numerical modelling that in most of the simulated cases the optimum ratio is 10, which was found to be dependent on inlet design and independent of solar radiation. For roof solar chimney, Du et al. (2011) concluded based on numerical modelling that the optimal ratio between chimney length and cavity gap is 12. For solar collector above the roof, the ratio between cavity length and hydraulic diameter must be greater than 15 to ensure a developed flow, and the ratio between stack height and width should be less than 7 if the airflow within the solar chimney is to be two-dimensional.

Zamora and Kaiser (2009) obtained numerically that the higher value of Rayleigh number, the lower value of the optimum ratio. The ratio was also found to be determined by inlet area and solar radiation.

iii. Solar radiation

Solar chimneys are generally considered to be unsuitable for regions with insufficient insolation or hot-arid climates. However, AboulNaga and Abdrabboh (2000) improved the chimney night ventilation performance by integrating a wall and a roof solar chimney. The results showed that the air flow rate was three times more than that of a roof solar chimney alone. The system was installed on a single house in Al-Ain, UAE. The optimum wall chimney height corresponding to the maximum air flow rate (nearly 2.3 m³/s) was 3.45 m

with an inlet height of 0.15 m. An ACH number up to 26 was achieved for a flat volume 321 m³. It is high enough to overcome the high-cooling load for a building in hot climate.

iv. Environment

Koronaki (2013) used EnergyPlus software to investigate three conventional solar chimneys. The first model is a solar chimney with the duct formed between the double glazed transparent cover and the absorbing wall. The second one is a solar chimney with the duct attached behind the double glazed absorbing wall and third model is solar chimney with the duct located in between the two double glazed absorbing walls, one facing eastward and the other westward, or southward and northward, accordingly. The result showed that the cooling power performance significantly depends on its location and orientation. It was found that for a typical solar chimney of 3 m high and 0.1 m wide with aerial hole of 0.2 m, facing southward, the cooling power performance at night is 3.27–10MJ/m per day. In the second and third models, it is 14.07 MJ/m per day southward. The second model facing west created an air flow rate of 98% as much as the first model facing south.

(c) Previous works

i. Computational Analysis

Lee and Strand (2009) concluded that chimney height, solar absorptance and solar transmittance turned out to have more influence on the natural ventilation improvement than air gap width and solar chimneys have more potential for cooling than for heating.

ii. Experimental Analysis

Experimental work has been carried out by Afonso (2000), who used test cells. Gan (1998) used these works to validate a CFD simulation model, which achieved a difference of only 2% between measured values and computer predictions. Data presented by Bouchair (1994) have also been used for validation purposes. Sparrow and Azevedo (1985) found, from experiment, that the natural convection between two plates reduces dramatically for a channel width of the same order of magnitude as the boundary-layer thickness. According to Andersen (1995), the channel width for solar chimneys should be at least 4.7 cm. The airflow rate increases for larger cavity widths up to 0.2–0.3 m. For wider cavities, Bouchair (1994) found that a back-flow developed in the middle of the cavity.

Zhai et al. (2005) found back-flow in an experimental set up with a 0.2 m gap. However, Gan (1998) claims rising flow rates for cavities larger than 0.3 m where the inlet breadth is the same size as the cavity width. Bends in the system cause additional pressure losses due to friction, and may also influence the flow along the heated surfaces and affect the thermal performance. Afonso (2000) demonstrated that increased thermal storage reduced the day-time flow but increased the night-time flow, as anticipated. The storage effect increases up to a thickness of 10 cm of brick, but beyond that thickness there is no significant change. Miyazaki et al. (2006) claimed that there is change up to 0.3 m thickness. Experimental work by Charvat et al. (2004) showed an increase in night-time air flow when thermal mass was added. They also showed that a solar chimney during the day gave, on average, 25% greater air flow than a conventional non-solar chimney. It is believed that there was a significant effect from the wind in both cases. The use of additional thermal mass was not investigated here.

Afonso (2000) found it essential to insulate the outside walls of the chimney in order to achieve solar efficiency: a thickness of 5 cm was considered to be adequate. Gan (1998) found that using double glazing on the cover increased the flow rate by 11%, where the chimney is also used in winter for heating (Trombe-wall type) then this would be most beneficial, but, for summer cooling only, the additional cost was not deemed worthwhile.

iii. Numerical Analysis

Having investigated the effect of different parameters on the performance of solar chimney system, Khedari et al. (2003) developed a numerical model to study the effect of different types of solar chimneys and their performance. They concluded that solar chimneys influence the air flow production. It was found that with solar chimney, room temperature reaches ambient temperature due to the natural ventilation created by solar chimney.

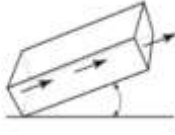
Mostafa Rahimi et al. (2011) investigated a combination of two natural ventilation methods. One of the method is based on air ventilation through a single or many openings found on a vertical wall through buoyancy effect whereas the other method involves the air movement through a vertical vent placed on the roof of an enclosure. The air flow velocity was the parameter being measured as an evaluation for the ventilation rate. A control was set up with no use of vent and eventually compared with repetitive experiments based on use of

vents. As a result, the air flow rate for the combined ventilation situation was reasonably predicted by the physical model proposed in his study.

2.2 Inclined roof chimney

(a) Mathematical models

The table below shows the main type of configurations for the inclined roof chimney type.

Typical Mathematical Models for Solar Chimney			
Reference	Year	Schematic	Equation
Shi et al.	2016		$V = w(\sin \theta)^{1/3} q^{1/2} d^{0.7} H^{2/3}$
Afonso and Oliveira	2000		$V = \frac{A_{out} \sqrt{2\alpha g (T_c - T_o) H}}{\sqrt{K_{in} \frac{A_{out}^2}{A_{in}} + K_{out} + f \left(\frac{H}{d}\right)}}$
Bansal et al.	1993		$V = C_d A_{out} \sqrt{\frac{2(T_c - T_o) g H \sin \theta}{T_o (1 + A_r^2)}}$

Source: Determining the influencing factors on the performance of solar chimney in buildings, Long Shi (2018)

(b) Influencing factors

i. Inclination angle

Zhai et al. (2005) investigated the use of a solar air collector for space heating and cooling in Shanghai, China whereby he found that the optimum collector inclination angle was 45° and a balance between air temperature rise and air-flow rate should be done to obtain maximum heat for space heating mode. The length of the solar air collector was recommended to be about 1 m.

Xinyu Zha et al. (2017) investigated experimentally and numerically the performance of a full-scale solar chimney installed in a real building in the region of Shanghai-China. Results indicate that the use of solar chimney for building ventilation in Shanghai permits to ensure

an energy saving rate in the order of 14.5% during the period from April to October. Bernardo Buonomo et al. (2015) studied numerically the effect of glass wall inclination of a solar chimney on the convective-radiative heat transfer in a building. Results show that the greatest thermal performance of the solar chimney is achieved at the highest investigated inclination angle.

ii. Environment

Aja et al. (2013) investigated the effect of wind speed and wind direction on the performance of an inclined solar chimney facing to the south. It was found that the wind speed had a great effect on the convective heat loss via the walls and the cover to the ambient. Nasirivatan et al. (2015) studied the influence of the Corona wind on the performance of solar chimney, showing the beneficial influence of the electro hydrodynamic force in improving the output power.

2.3 Vertical roof wall

A high cavity is beneficial to enhance its performance with the increased pressure difference and heat gain. A power function is shown between airflow rate and cavity height with an exponent between $1/2$ and $2/3$, also applicable to multiple storeys building. An appropriate cavity gap is essential for the performance of a solar chimney. An optimum cavity gap of 0.2–0.3m is generally applicable, although other factors such as inlet area, chimney height, and inclination angle should be considered. An equal area for inlet and outlet is a good way to improve the performance of a solar chimney. For unequal openings, increasing outlet area seems to be more efficient comparing to the inlet.

2.4 Inclined roof chimney

Inclination angle is the key factor to roof solar chimney, and an optimum inclination angle of $45\text{--}60^\circ$ is suggested considering the latitude of the building. The optimum angle should be considered with a balance between stack pressure and convective heat transfer. Due to this reason, for a solar chimney at a specific location, the optimum inclination angle is higher than the angle receiving the maximum solar radiation. The position of the opening seems is not a

primary factor affecting the solar chimney performance, while skylight shows a slightly better performance compared to window and door. A solar collector is used to increase the amount of heat gains from the solar radiation. Therefore, design features such as increasing the area of collector plate and using materials with high absorptivity and low thermal conductivity can improve performance.

2.5 Proposed Model

The present research study involves CFD modelling, using the ANSYS- FLUENT software to simulate the flow of the chimney. The geometry is created in ANSYS using SpaceClaim. The geometry is shown in Figure 2. The overall height of the solar chimney was 2.95 m and the width 0.95 m.

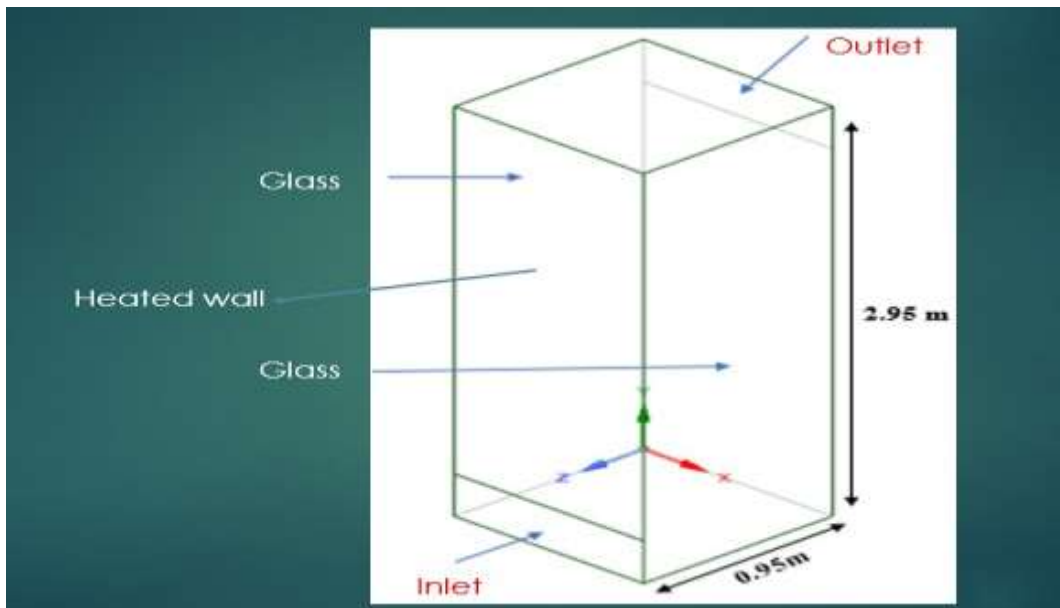


Figure 2: The geometry of the solar chimney created in ANSYS SpaceClaim

The next step of CFD simulation is the discretization of the computational domain and mesh generation. Thereafter the flow inside the solar chimney cavity is simulated to understand the basic parameters and functioning of the system. A solar chimney with a heated wall was considered. The heated wall consist of black aluminium cladding and the three remaining sides consisted of transparent glass panes. The properties of the material are given in Table 3.

Table 3: Material Properties

Material	Thickness/m	Density/ (kg/m ³)	Specific Heat/(J/kg-K)	Thermal conductivity/(K-1)
Glass	0.006	2700	700	1.4
Aluminium	0.006	2719	871	202.4

In the simulation model, the air properties are assumed to be constant. The ambient air temperature was taken assumed to be 300 K (27 °C) with density: 1.225 kg/m³, Viscosity: 1.7894×10⁻⁵ kgm⁻¹s⁻¹ and thermal expansion coefficient of 0.00336 K⁻¹. The Boussinesq approximation has also been assumed for the buoyancy force arising from density variation as a result of temperature change. A Reynolds-Averaged Navier-Stokes (RANS) formulation is used in this study. Two openings are used in this model. A solar chimney inlet opening has been assigned with pressure inlet. The solar chimney outlet opening has been assigned with ambient conditions based on normal atmosphere. The fluid has been considered at atmospheric pressure with a constant gauge value of P = 0 Pa. The heated wall of the solar chimney will be assigned different heat flux values during the simulation scenarios. Different constant values of solar heat flux will be considered to study the effect on the natural ventilation. The different boundary conditions are described below:

Pressure inlet

The pressure boundary conditions are applicable when neither the flow rate nor the flow velocity are known. The treatment of pressure inlet boundary conditions can be described as a loss-free transition from stagnation conditions to the inlet conditions. For incompressible flows, this is accomplished by application of the Bernoulli equation at the inlet boundary. In incompressible flow, the inlet total pressure and the static pressure, p_s , are related to the inlet velocity via the Bernoulli equation:

$$p_0 = p_s + \frac{1}{2}\rho v^2$$

Where p_0 is the total pressure of the fluid at the inlet plane and p_s is the static pressure.

Pressure Outlet

Pressure outlet boundary conditions require the specification of a static (gauge) pressure at the outlet boundary. A backflow condition occurs if the flow reverses direction at the pressure outlet boundary during the solution process.

Velocity inlet

Velocity at the boundary condition is used to define the flow velocity at flow inlet. This boundary condition is mainly used for incompressible flows. The inflow velocity is specified by the velocity magnitude and direction, the velocity components, or the velocity magnitude normal to the boundary. The velocity inlet is used to compute the mass flow into the domain through the inlet and to compute the fluxes of momentum, energy through the inlet. The mass flow rate entering a fluid cell adjacent to a velocity inlet boundary is computed as:

$$\dot{m} = \int \rho \vec{v} \cdot d\vec{A}$$

Where \dot{m} is the mass flow rate, ρ is the density of the fluid, \vec{v} is the velocity vector.

Constant temperature

When a fixed temperature condition is applied at the wall, the heat flux to the wall from fluid cell is computed as:

$$q = \frac{h_f(T_w - T_f)}{\Delta n} + q_{rad}$$

Where h_f = fluid-side local heat transfer coefficient, T_w = wall surface temperature, T_f = local fluid temperature and q_{rad} = radiative heat flux, Δn = distance between wall surface and the solid cell centre. The fluid-side heat transfer coefficient is computed based on the local flow-field conditions. Heat transfer to the wall boundary from a solid cell is computed as:

$$q = \frac{k_s(T_w - T_s)}{\Delta n} + q_{rad}$$

Where k_s = thermal conductivity of the solid, T_s = local solid temperature, Δn = distance between wall surface and the solid cell centre.

Constant heat flux

When a constant a heat flux boundary condition at a wall, the heat flux at the wall surface is used to determine the wall surface temperature adjacent to a fluid cell as:

$$T_w = \frac{q - q_{rad}}{h_f} + T_f$$

2.4 Heat transfer

Heat transfer can be defined as the exchange of energy between material bodies due to a difference in temperature. Heat conduction is the transfer of energy which occurs in a stationary medium, which can either be a solid or a fluid, when there is a temperature gradient in the medium.

2.5 Efficiency of solar chimney

Air is continuously exchanged between buildings and their surroundings as a result of mechanical and passive ventilation and infiltration through the building envelope. The rate at which air is exchanged is an important property for the purposes of ventilation designs expressed in air changes per hour (ach). If a building has an air change rate of 1 ach, this means that all of the air within the internal volume of the building is replaced over a 1 hour period. The air change per hour can be calculated as follows:

$$ACH = 3,600 \times q/V$$

Where AC H is the Air changes per hour (ach), q is air flow rate (m³ /s), V is Volume of the room (m³).

3. Experimental Set-up of a solar chimney

An experimental setup was implemented at the University of Mauritius (UoM) on the roof of the Machine shop in Reduit. The aim is to simulate a vertical solar chimney using a design which offers ease of installation over a roof or against a wall, and can readily fit into the local construction culture. The traditional black painted, high thermal mass was not considered as it has been deemed in the past to be not aesthetically appealing and will entail important structural implications when installed over the roof.

The setup is shown in Figure 3. It is made up of an aluminium frame structure with glass panes on three sides and black-coloured aluminium cladding on the fourth side, which acts as a heat concentrator for the internal cavity of the system. The overall dimension of the solar chimney is of 0.95m length by 0.95m wide by 2.95m tall. The glass pane thickness is 6mm. The set-up is composed of 4 openings: two located at the bottom and two is located at the top of the solar chimney. A small door is also included in the design for ease of movement in and out of the solar chimney for maintenance and installation purposes. The aim of the experimental set-up is to record air velocities and temperature at the inlet and outlet of the solar chimney to be used in to validate the CFD model.

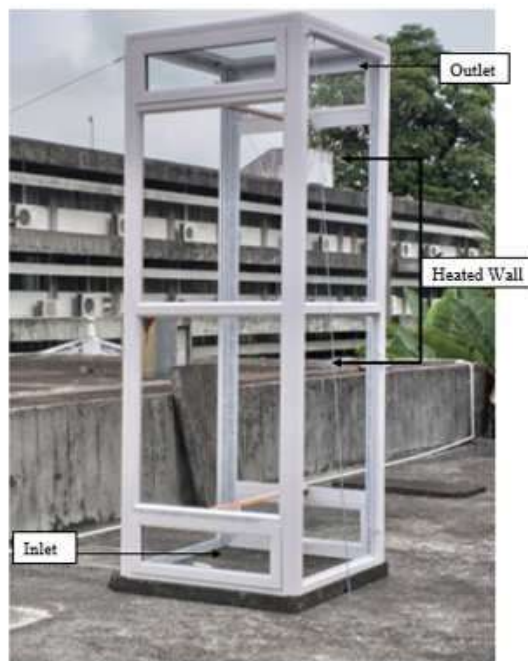


Figure 3: Experimental setup of solar chimney

3.1 Instrument used in assessing important parameter in solar chimney

3.1.1 Flow sensor

The T-DCI-F300-1x3 sensor has an air velocity and temperature sensor which is used to measure the air velocity and temperature inside the solar chimney. The sensor is designed with conformal coated electronics and sealed enclosures. Figure 4 shows the T-DCI- F300-1x3 sensor.



Figure 4: Air Velocity and Temperature Sensor (T-DCI-F300-1x3)

The velocity range of this sensor is up to 1 m/s and an operating temperature range of 0 °C to 100 °C. Velocity measurements can be used to reveal the performance of an airflow system like the solar chimney. A data logger and a power adapter is required to measure the velocity and temperature at a specific location. A HOBO 4-Channel Analog Data Logger (UX120-006M) (shown in Figure 5) and a HOBO 4-Channel External Data Logger (U12-008) (shown in Figure 6) are used to record the air velocity and temperature.

The air velocity sensor has been calibrated with a calibrated hand-held anemometer to ensure accuracy of velocity measurements. To calibrate a sensor, a reference air velocity sensor is used. A fan is used in a honey-comb to generate a laminar flow. A large distance between the fan and the air velocity is required so that it allows a measurement of the range of the equipment which is less than 1 m/s.



Figure 5: HOBO 4-Channel Analog Data Logger (UX120-006M)



Figure 6: HOBO 4-Channel External Data Logger (U12-008)

Two sensors are calibrated simultaneously as the same height. In this way, four sensors were calibrated. The 1st sensor was found to be properly calibrated, the 2nd sensor needs to be adjusted by +0.08 m/s, the 3rd sensor was found to be calibrated and 4th sensor need to be compensated by +0.12 m/s. The temperature sensors were also calibrated using a reference temperature sensor. The 1st sensor was found to be properly calibrated, the 2nd sensor needs to be compensated by -0.05 °C, the 3rd sensor was found to be properly calibrated and 4th sensor had to be compensated by -0.30° C.

4. Simulation Results and Discussion

The numerical analysis is carried out on a three-dimensional model and the governing equations are given by the $k - \varphi$ turbulence model. The results are provided in terms of temperature distributions and air velocity at the inlet and outlet. Different constant solar heat fluxes have been applied on the system to study the buoyancy effect created. A range of 100 W/m^2 and 1000 W/m^2 was considered for the heat flux to cover the range of values of solar radiation the system will be exposed to under varying solar angles and sky conditions. For a heat flux of 100 W/m^2 , the velocity, temperature and pressure contours are illustrated in Figure 7 to Figure 9.

The inlet temperature was set at 303.15 K (30° C). The contours of the temperature distributions are shown at steady state solution. The density change is the cause of the fluid buoyancy, causing the air to move up through the chimney as depicted by the flow vectors. The temperature distribution inside the chimney varied from 28.4° C to 35.9° C , with the velocity at the inlet is smaller than that of the outlet. The velocity distribution lies between 0.04 m/s to 0.82 m/s . A negative pressure was observed at the inlet and the pressure distribution lied between -0.15 Pa to 0.49 Pa .

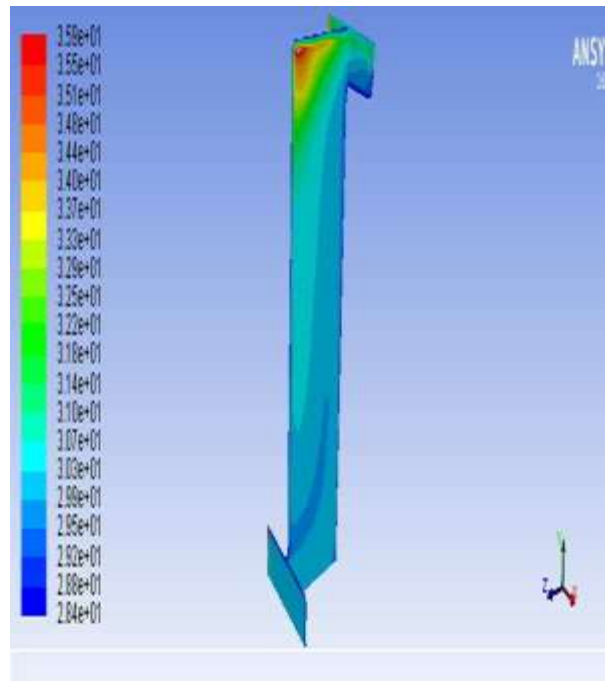


Figure 7: Temperature contour of the solar chimney with constant heat flux on 100 W/m^2 .

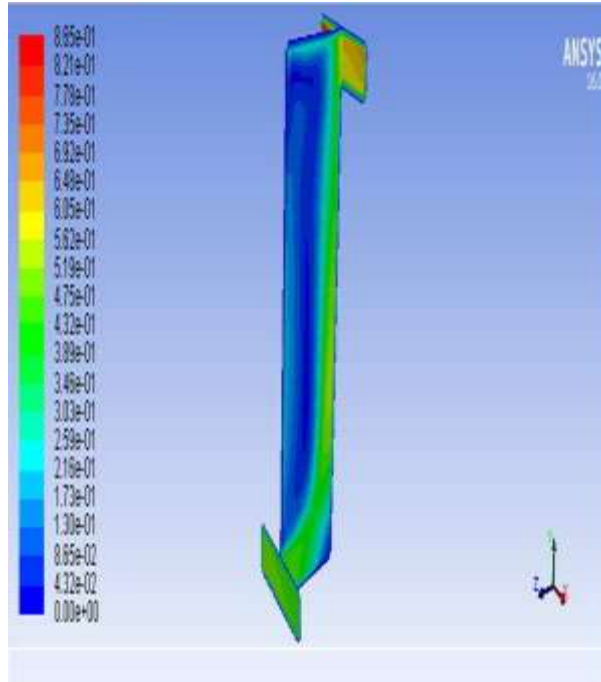


Figure 8: Velocity contour of the solar chimney with constant heat flux on 100 W/m^2 .

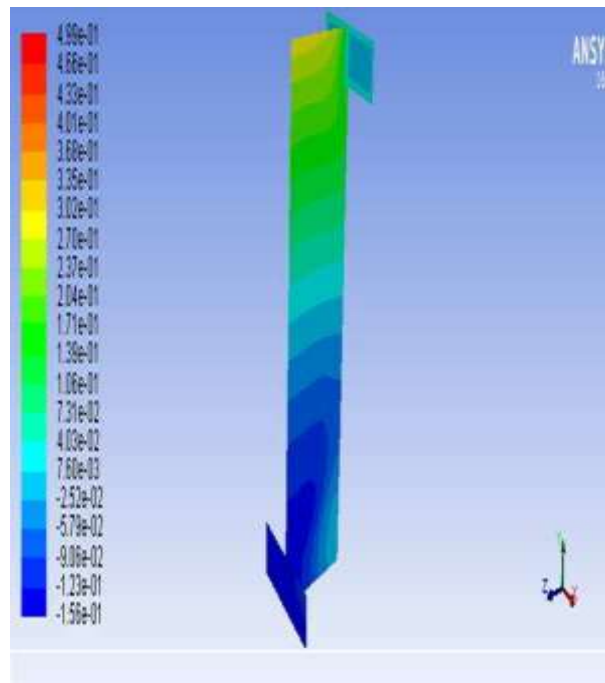


Figure 9: Pressure contour of the solar chimney with constant heat flux on 100 W/m^2 .

Next, a variation of the heat flux from 100 W/m^2 to 1000 W/m^2 was configured on the heated wall in turn to investigate the effect on the inlet and outlet flow parameters of the solar chimney. Figure 10 shows the temperature distribution of the outlet at various heat flux on the heated wall.

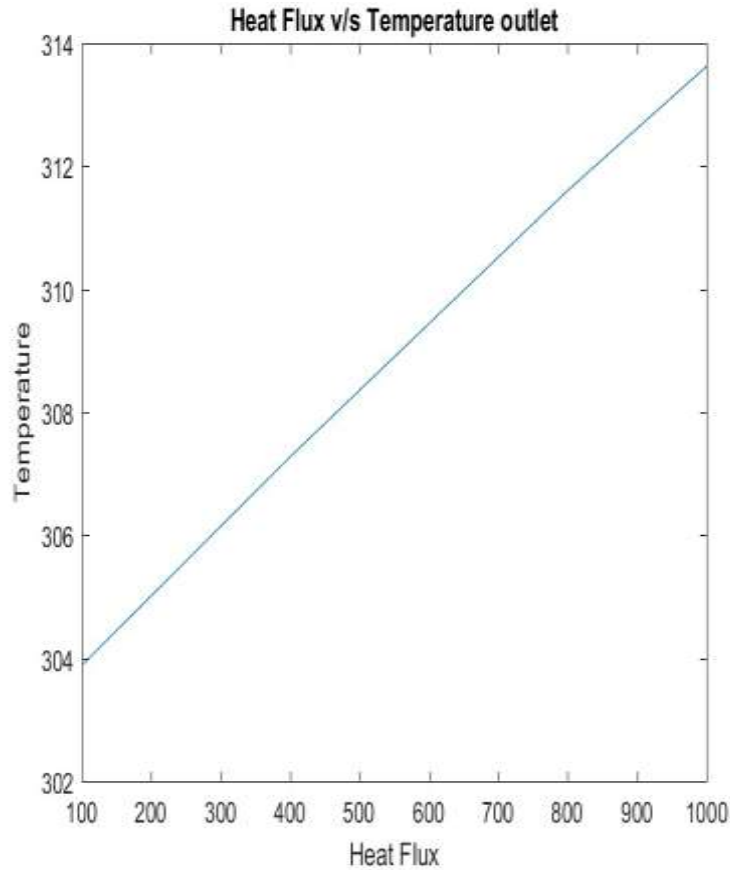


Figure 10: Temperature distribution of the outlet at variation of heat flux from 100 W/m² to 1000 W/m².

A linear increase in the temperature values of the outlet was observed. Figure 11 and Figure 12 below show the velocity measured at inlet and outlet at various heat fluxes. The distribution of the pressure inlet at various heat fluxes is shown in Figure 13.

It can be observed from the graph that the pressure at the inlet decreases progressively as the heat flux increases. Next, the effect of reducing the size of the solar chimney was investigated to assess the efficiency and the flow parameter. The geometry of the reduced size of the solar chimney is shown in Figure 14. Similar profiles for the outlet temperature, inlet velocity, outlet velocity and inlet pressure with various heat fluxes on the heated wall were generated. Six different heat flux were considered namely 100, 200, 400, 600, 800 and 1000 W/m².

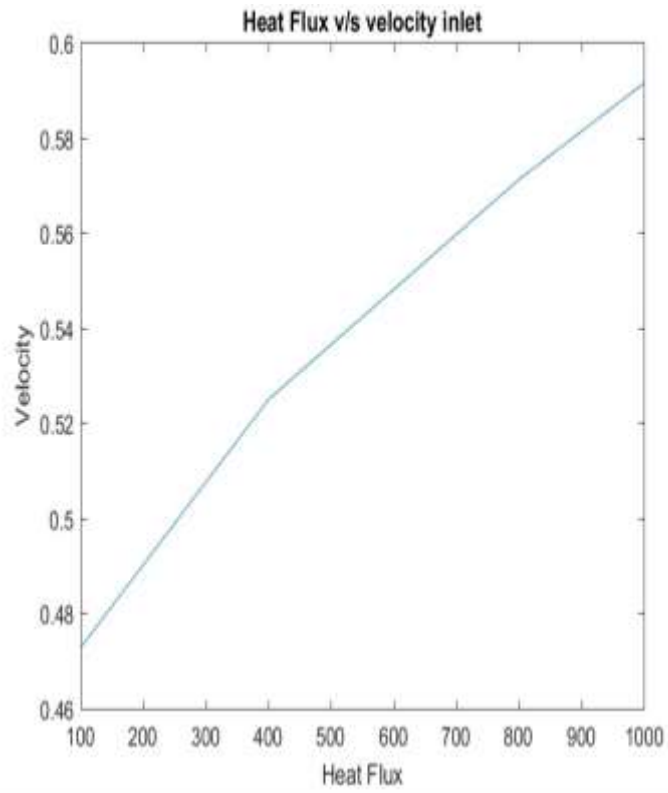


Figure 11: Velocity inlet distribution for variation of heat flux from $100 W/m^2$ to $1000 W/m^2$.

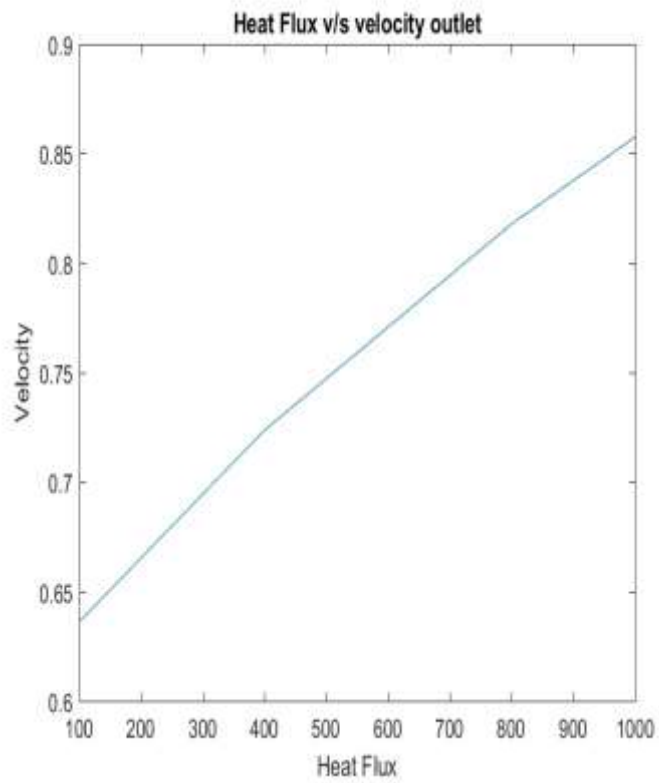


Figure 12: Velocity outlet distribution for variation of heat flux from $100 W/m^2$ to $1000 W/m^2$.

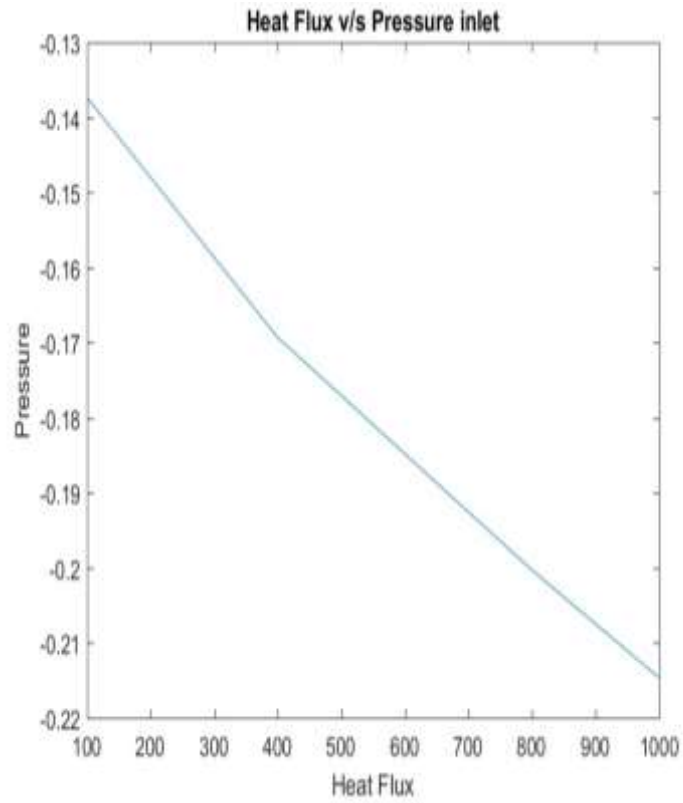


Figure 13: Pressure inlet distribution for variation of heat flux from 100 W/m² to 1000 W/m²

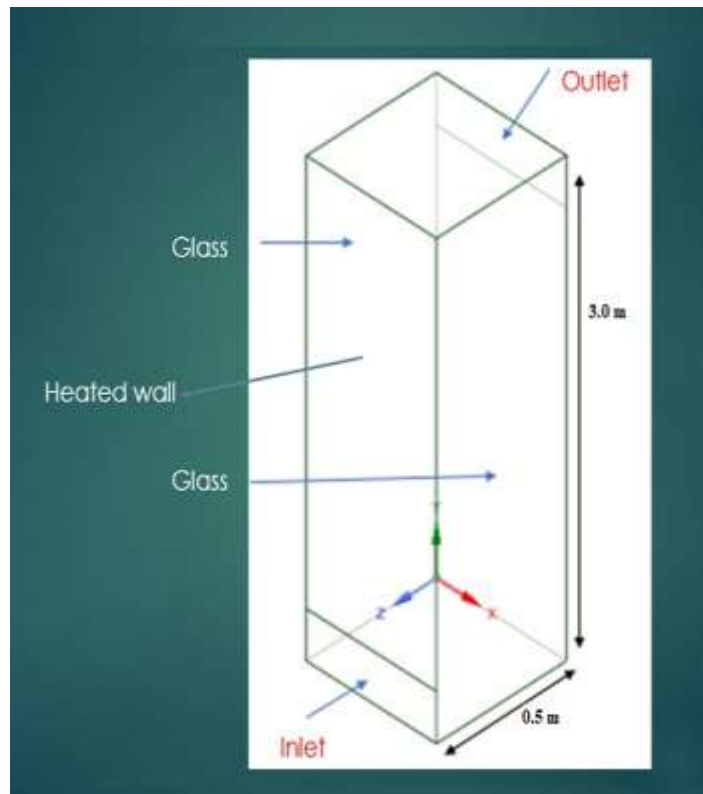


Figure 14: Geometry of solar chimney with size 0.5m by 0.5m by 3m.

Figure 15 shows the outlet temperature (in Kelvin) for various heat fluxes.

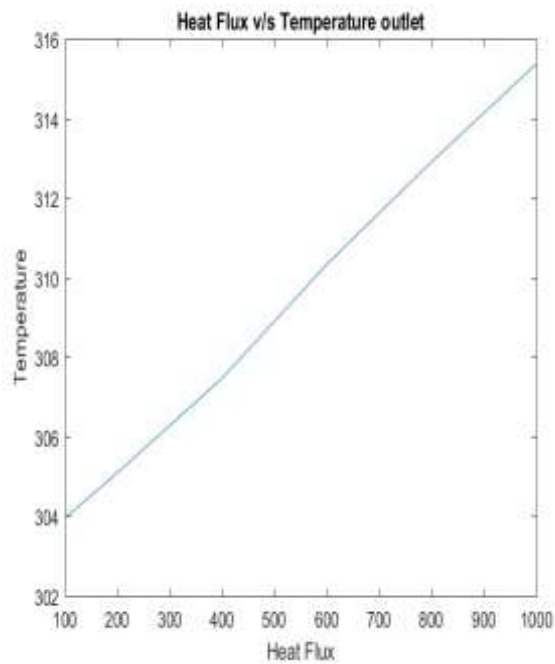


Figure 15: Temperature distribution of the outlet with a solar chimney with size 0.5m by 0.5m by 3m

Figure 16 and Figure 17 below show the inlet and outlet velocities respectively for a solar chimney of size 0.5 m by 0.5 m by 3 m.

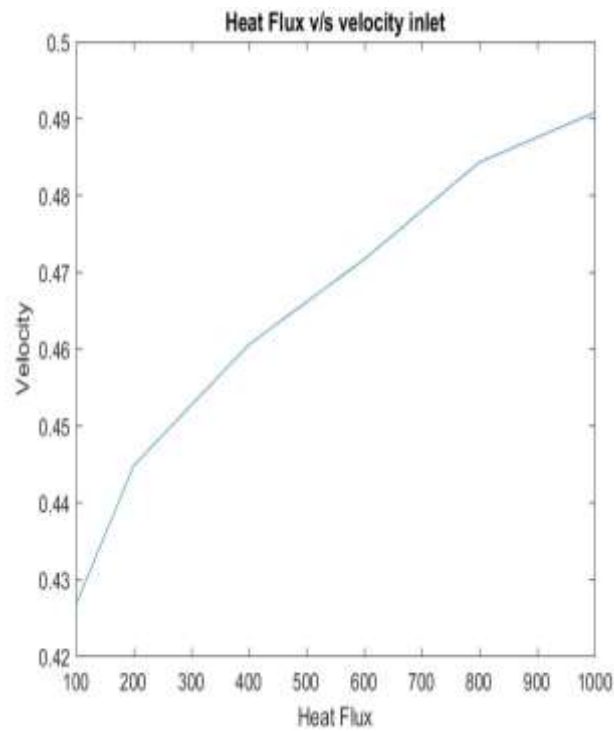


Figure 16: Velocity distribution of the inlet with a solar chimney with size 0.5m by 0.5m by 3m.

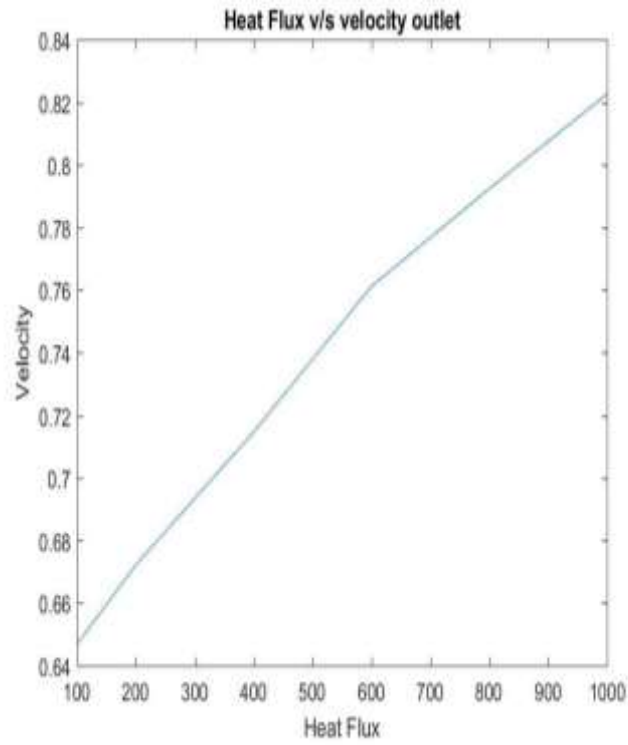


Figure 17: Velocity distribution of the outlet with a solar chimney with size 0.5m by 0.5m by 3m

Figure 18 shows the pressure inlet at various heat fluxes for a solar chimney of size 0.5m by 0.5 m by 3 m.

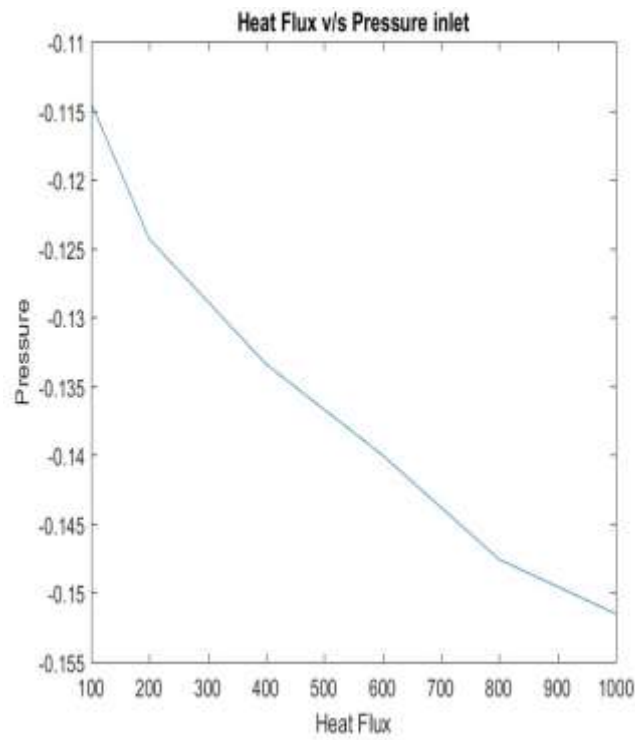


Figure 18: Pressure distribution of the inlet with a solar chimney with size 0.5m by 0.5m by 3m.

The ACH for a 5m by 5m by 3m room is plotted in Figure 19 at different heat fluxes for the solar chimney of dimension 0.95m by 0.95m by 2.95 m.

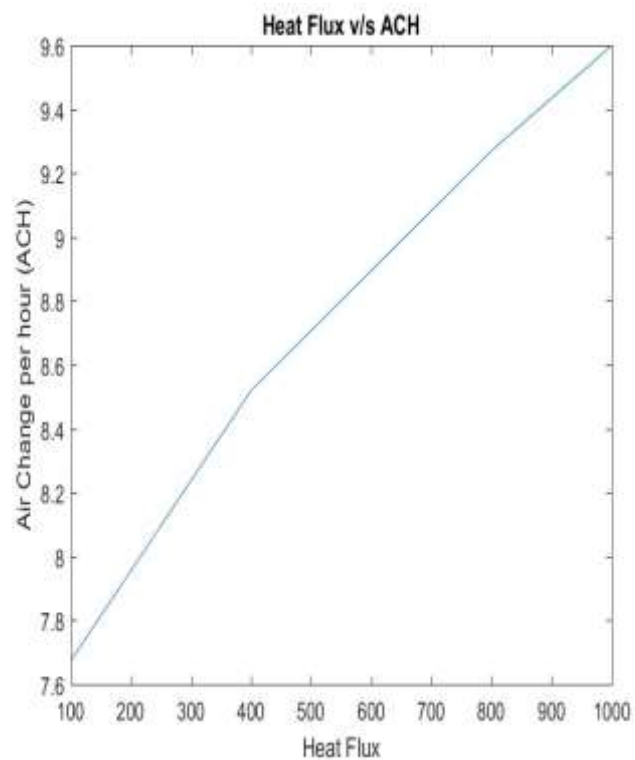


Figure 19: Air Change rate of a room 5m x 5m x 3m with a solar chimney with size 0.95m by 0.95m by 3m.

The ACH for a solar chimney of reduced size at 0.5m by 0.5m by 3 m is graphed in Figure 20 for a room of similar size as above. The ACH of different size of solar chimney, namely: 0.5m by 0.5m, 1m by 1m and 2m by 2m are compared, all of the same 3m height. The ACH at different heat fluxes for a room of 5m by 5m by 3m are plotted in Figure 21.

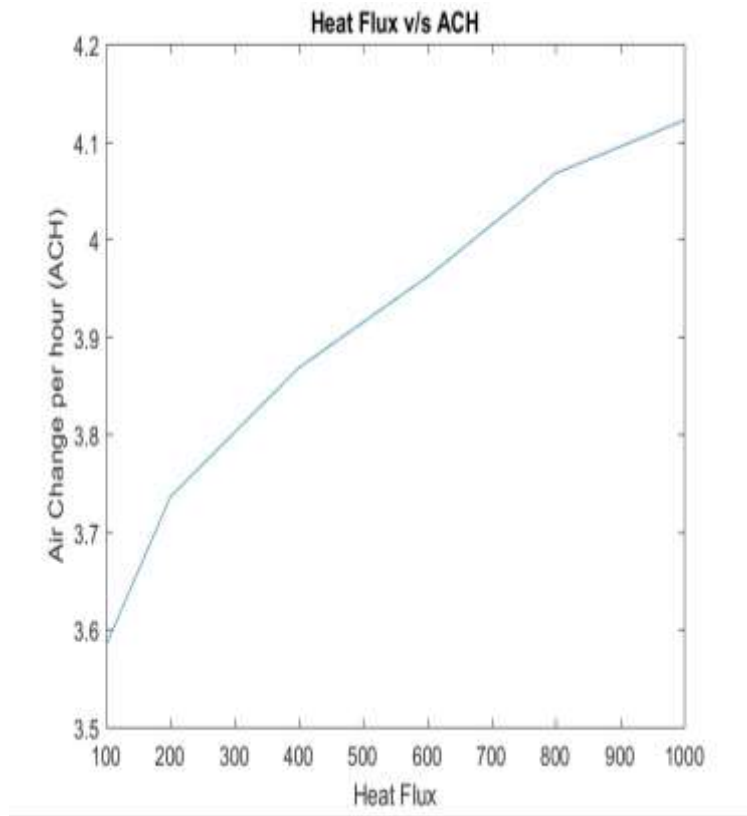


Figure 20: Air Change rate of a room 5m x 5m x 3m with a solar chimney with size 0.5m by 0.5m by 3m.

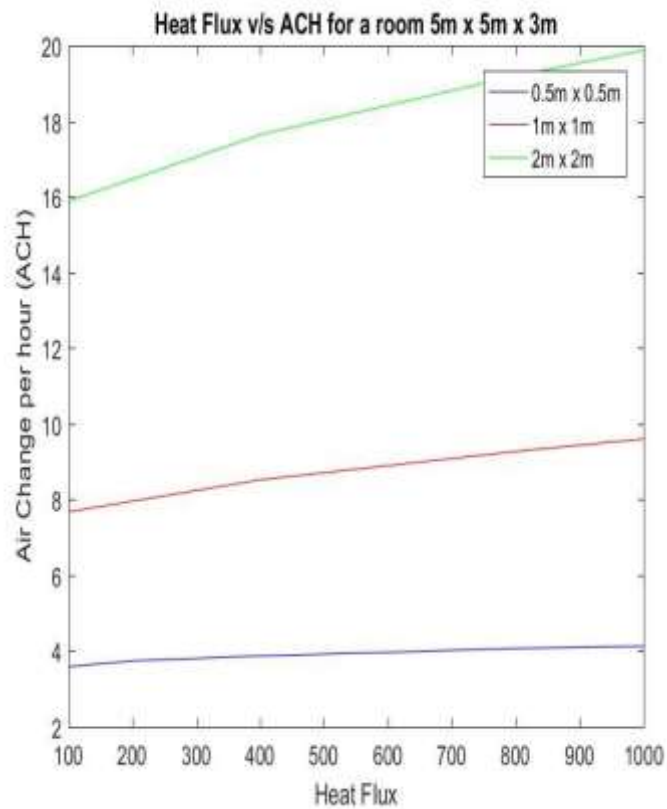


Figure 21: Compare the Air Change rate of a room 5m x 5m x 3m with a different size of solar chimney

As expected, the ACH increases with the size of the solar chimney. Next, the effect of increasing the dimension of the room on the ACH using different dimensions of solar chimney was investigated. The results are illustrated we investigate in Figure 22 for a room of dimensions 10m by 10m.

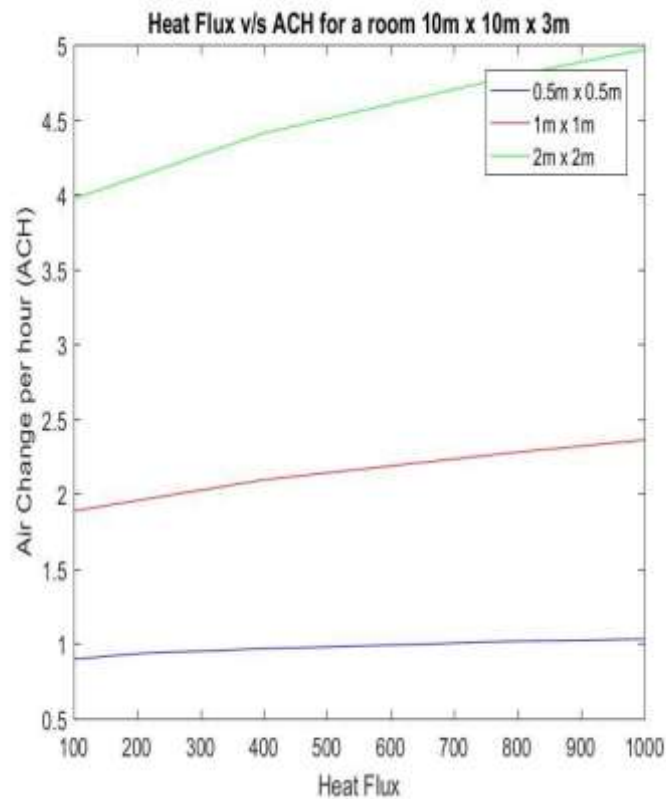


Figure 22: Compare the Air Change rate of a room 10m x 10m x 3m with a different size of solar chimney.

It was observed that increasing the size of the room by a linear factor of 2 decreases the ACH by a factor of 4. Next, the effect of velocity contour inside the interior space is considered.

The analysis of the thermal comfort of a naturally ventilated building of 5m by 5m by 3m with a solar chimney was analysed using Building Energy Simulation and Computational Fluid Dynamics with DesignBuilder. DesignBuilder also has an integrated Computational Fluid Dynamics (CFD) package. Anderson & Wendt (1995) defines CFD as the art of replacing the partial derivatives with discretized algebraic forms, which in turn are solved to obtain numbers for the flow field values at discrete points in time and space.

DesignBuilder models the Navier-Stokes equations for the continuity, momentum and energy. DesignBuilder solve these equations using a finite volume method and the user has the ability of choosing between 3 types of discretization namely upwind, hybrid and power Law scheme. In the DesignBuilder CFD package, a grid is automatically generated for the required model domain by identifying all contained model object vertices and then generating key coordinates from these vertices along the major grid axes.

A room of 5m by 5m by 3m is considered in Designbuilder with a window and the inlet of the solar chimney on adjacent sides of the room. The velocity distribution across the room was first studied. The flow inlet at the bottom of the house represents the inlet opening in the solar chimney created in ANSYS earlier. Designbuilder was applied to simulate the ventilation problem using the $k - \epsilon$ model solver at steady state. The velocity distribution inside the room is displayed at 3 different places Figure 23. The velocity was found to lie between 0 m/s to 0.41 m/s in the room.

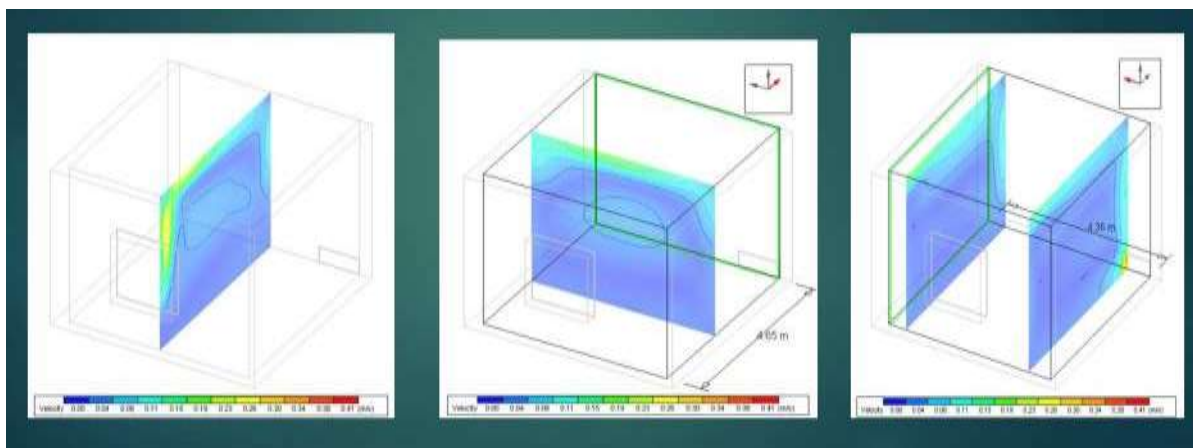


Figure 23: Velocity contour of a room 5m x 5m x 2.95m for a solar chimney of size 0.95m by 0.95m by 2.95m.

The flow with a reduced solar chimney size of 0.5m by 0.5m by 3m coupled to a room of 5m by 5m was simulated next in Designbuilder. The velocity contour across the room is computed and illustrated in Figure 24.

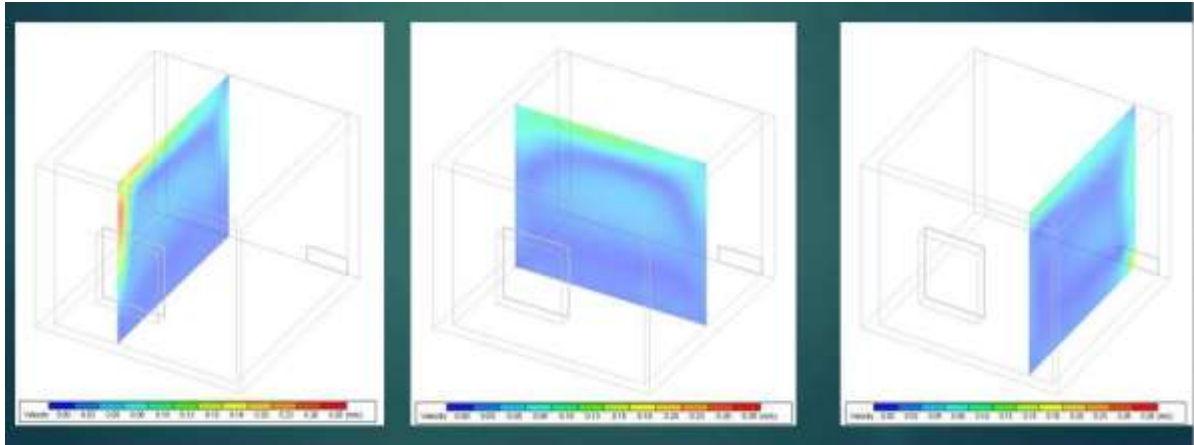


Figure 24: Velocity contour of a room 5m x 5m x 2.95m for a solar chimney of size 0.5m by 0.5m by 3m.

In this case, the velocity was found to range from 0 m/s to 0.28 m/s inside the room. The velocity was found to be higher near the windows, inlet of the solar chimney and near the ceiling. To see the effect on the thermal comfort, the velocity contour at heights of 0.5m, 1m and 1.5m on a horizontal plane were studied. Figure 25 shows the velocity contours obtained with a solar chimney of 0.95m by 0.95m by 2.95m and a room of size 5m by 5m by 2.95m.

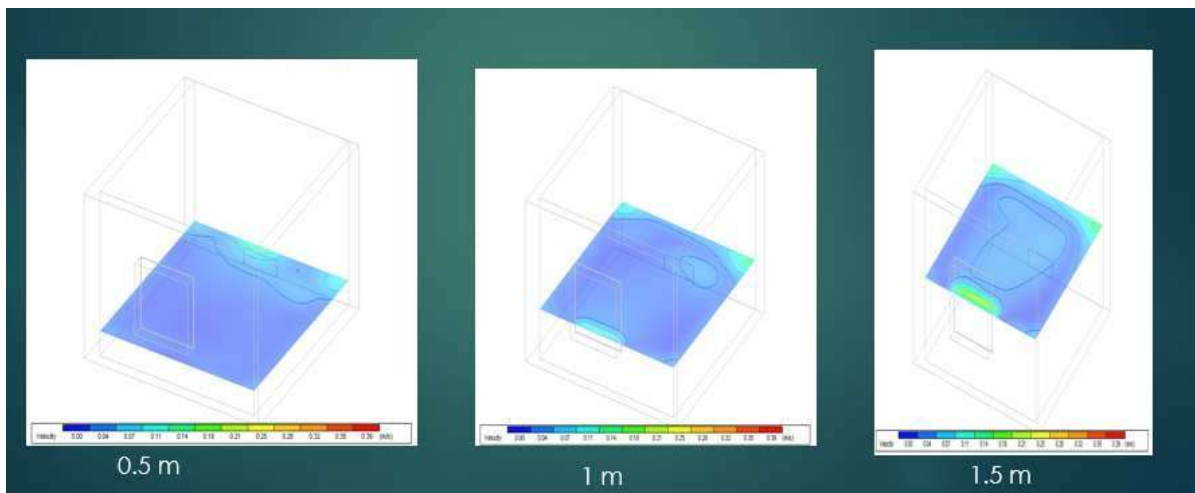


Figure 25: Velocity contour of a room 5m x 5m x 2.95m for a solar chimney of size 0.95m by 0.95m by 2.95m.

Figure 26 illustrates the velocity contours for a room size of 5m by 5m by 3m with a solar chimney of size 0.5m by 0.5m by 3m.

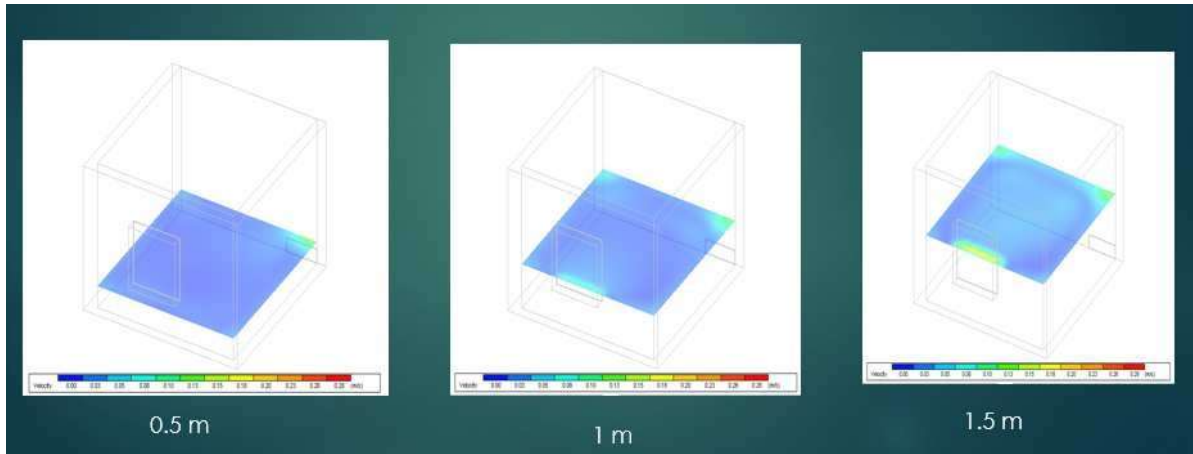


Figure 26: Velocity contour of a room 5m x 5m x 3m for a solar chimney of size 0.5m by 0.5m by 3

5. Experimental Results and Discussion

The diagram (Figure 27) below illustrates the location of the four flow/velocity sensors in the solar chimney prototype constructed and installed above the Machine Shop roof at the Faculty of Engineering at the University of Mauritius.

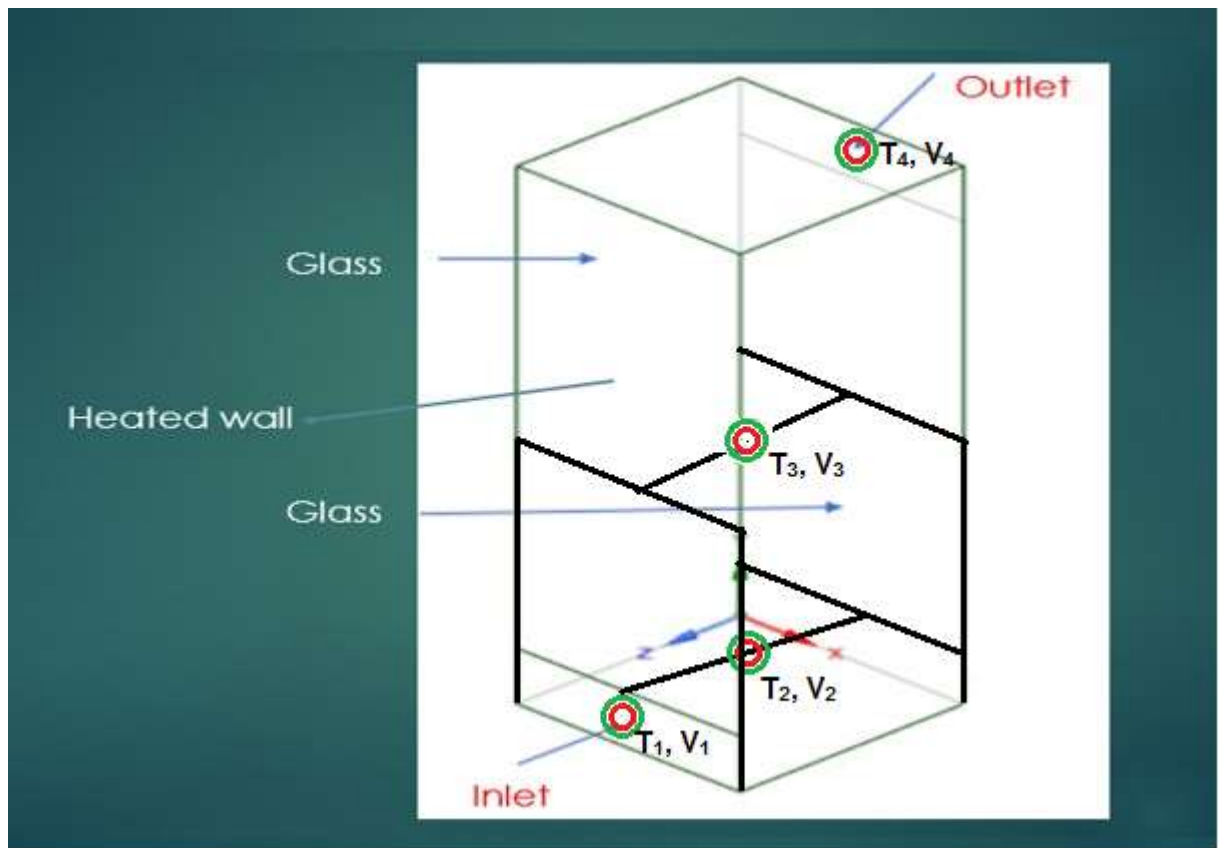


Figure 27: Flow/velocity sensor placement in solar chimney prototype

In addition to these four flow/velocity sensors, a weather station was installed next to the prototype to measure ambient temperature and wind speed, which are deemed important parameters to correlate to the internal measurements of the solar chimney. Moreover, the solar radiation was measured using a pyranometer. The temperature profiles of Figure 28 and Figure 29 show typical variations of the four temperature and velocity parameters as per Figure 27 above. It is observed that the temperatures at the inlet and outlet have lower temperatures as compared to T2 and T3, found inside the solar chimney prototype. The lower value for T1 is logical as this is the ambient, unheated air temperature, expected to be similar to the ambient temperature. However, a lower value for T4 is most probably caused due to mixing with external air. Indeed, as shown in Figure

29, the flow at location point 4 at the outlet shows more activity as compared to the other locations, confirming the influence of ambient air on the sensor at that location. The distribution of air flow velocities within the solar chimney is found to be between 0 and 1 m/s, hence comparable to what was measured in the CFD models.

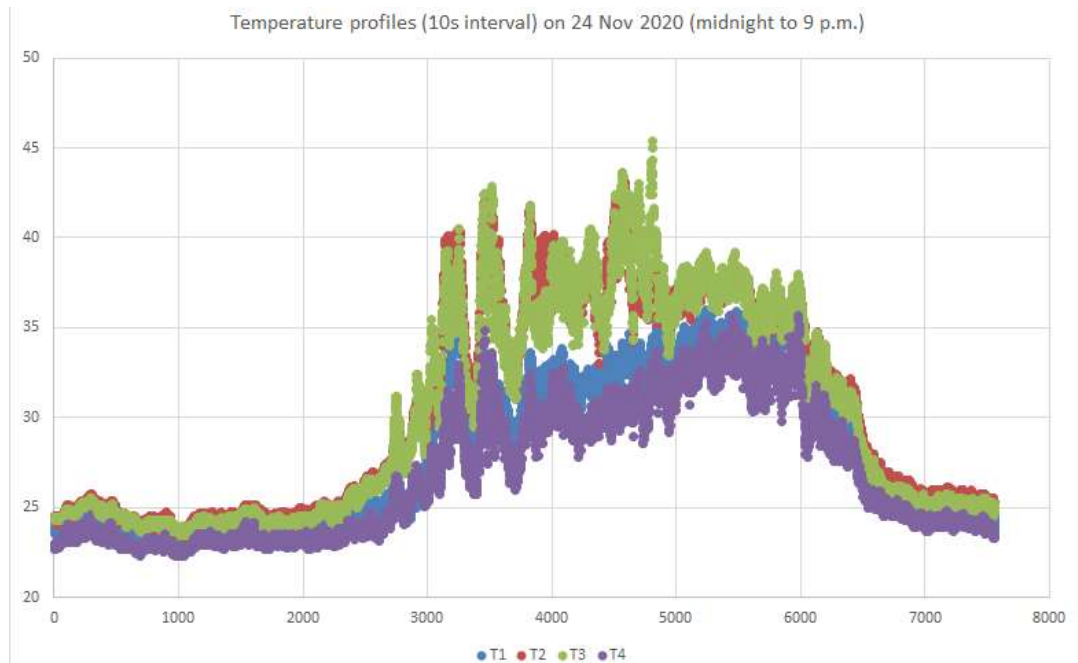


Figure 28: Typical temperature profile for summer period

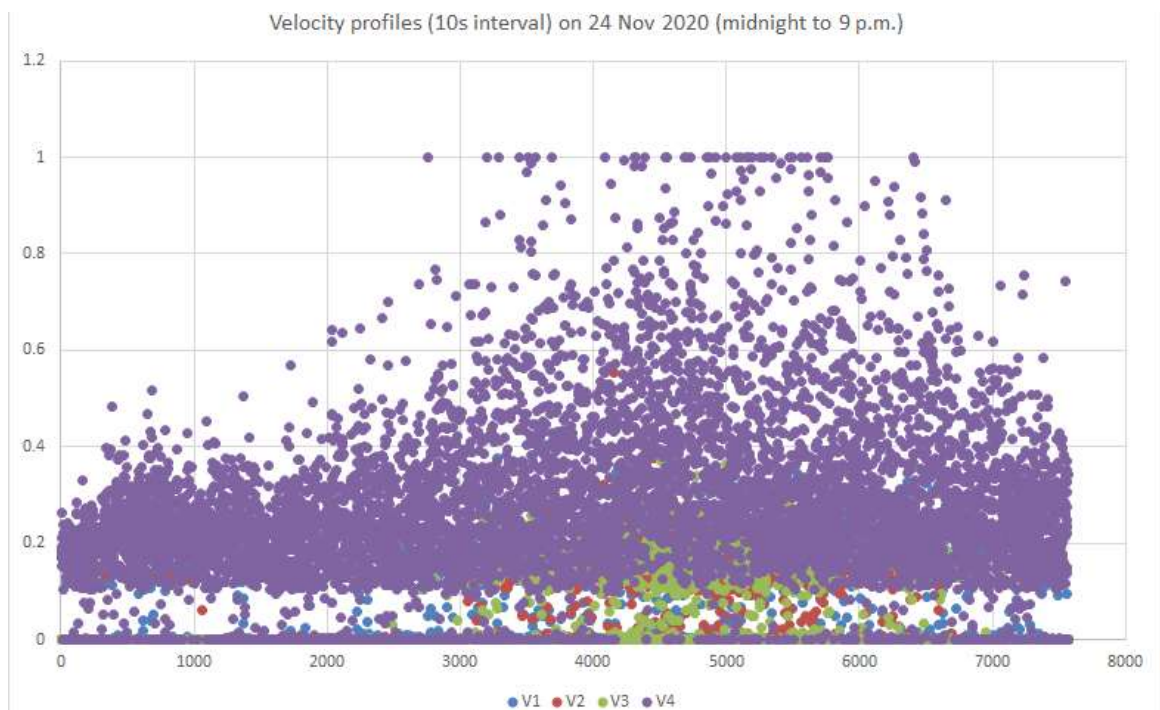


Figure 29: Typical velocity profile for summer period

Figure 30 and Figure 31 illustrate the typical profiles observed over winter periods, where the objective of this analysis is to assess the potential to shift the mode of operation of the solar from one of extracting air from the interior space using the buoyancy force created to one supplying warm air to the interior spaces of the building, which would be relevant in cold regions such as Vacoas and Curepipe during peak winter periods.

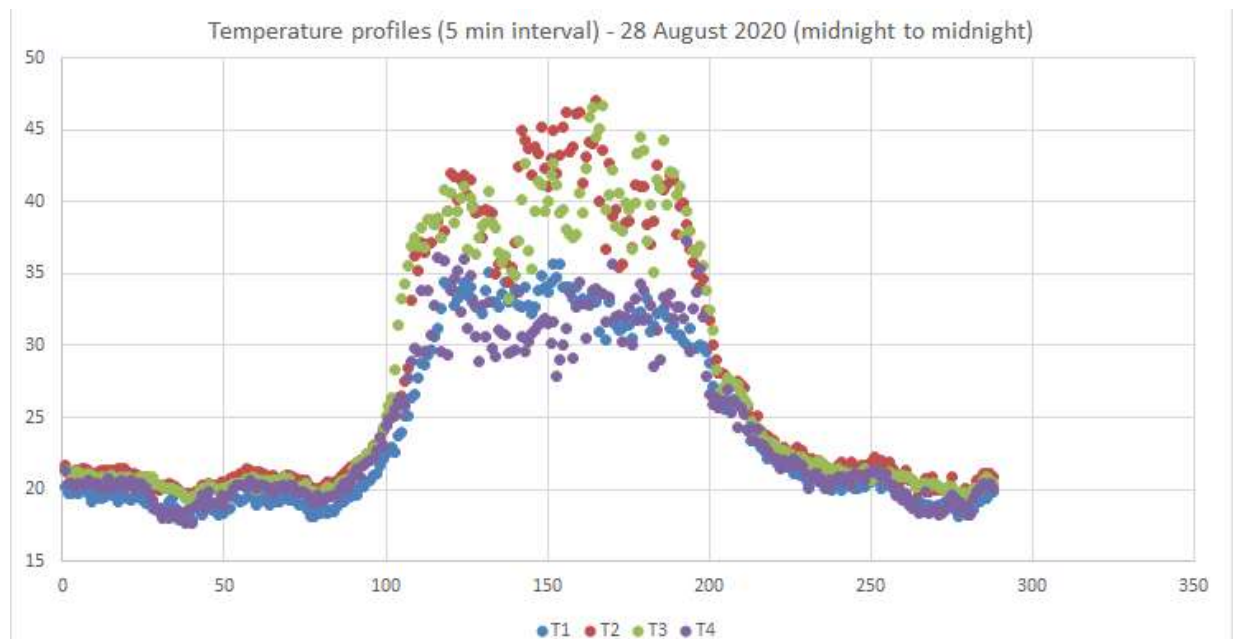


Figure 30: Typical temperatures in winter period

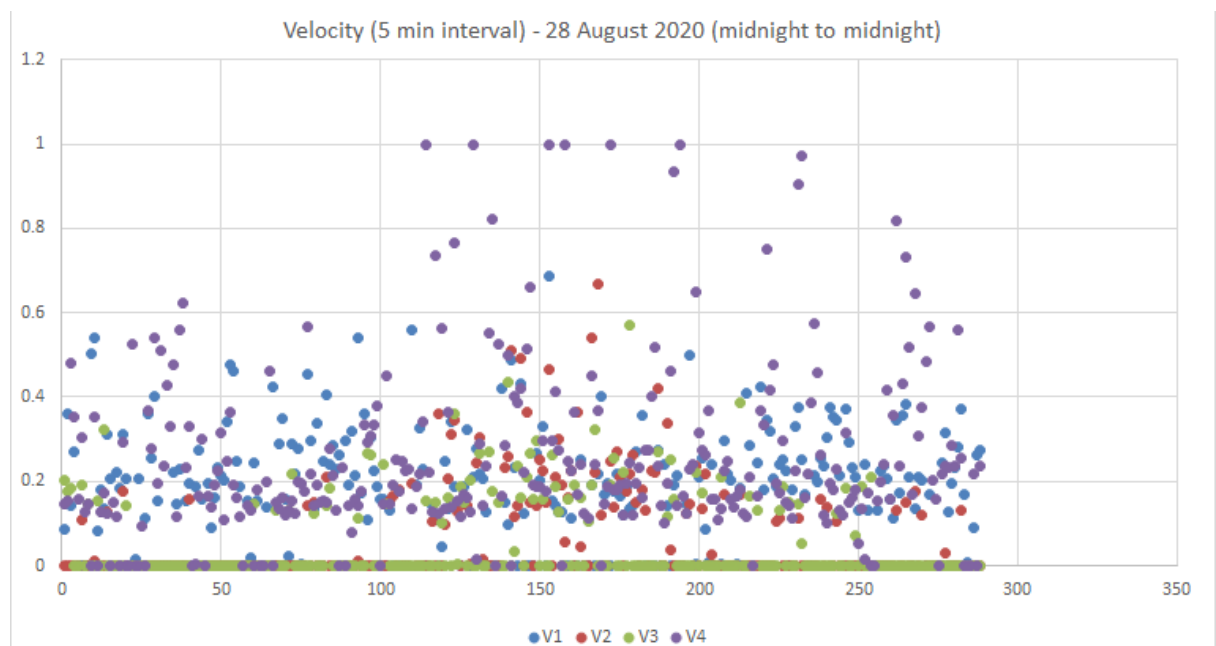


Figure 31: Typical velocity profiles in winter period

Since the buoyancy phenomenon of the solar chimney is caused by solar radiation, a period of the dataset was selected which has a high solar radiation, as measured by the pyranometer. The graph of Figure 32 shows the variation of the solar radiation from 16 December 2020 (10 a.m.) to 17 December 2020 (noon), clearly showing the day and night periods between these two days. The wind speed measurements from the weather station are also illustrated in Figure 33 for that same period as air movement created by wind is expected to affect the behaviour of the solar chimney.

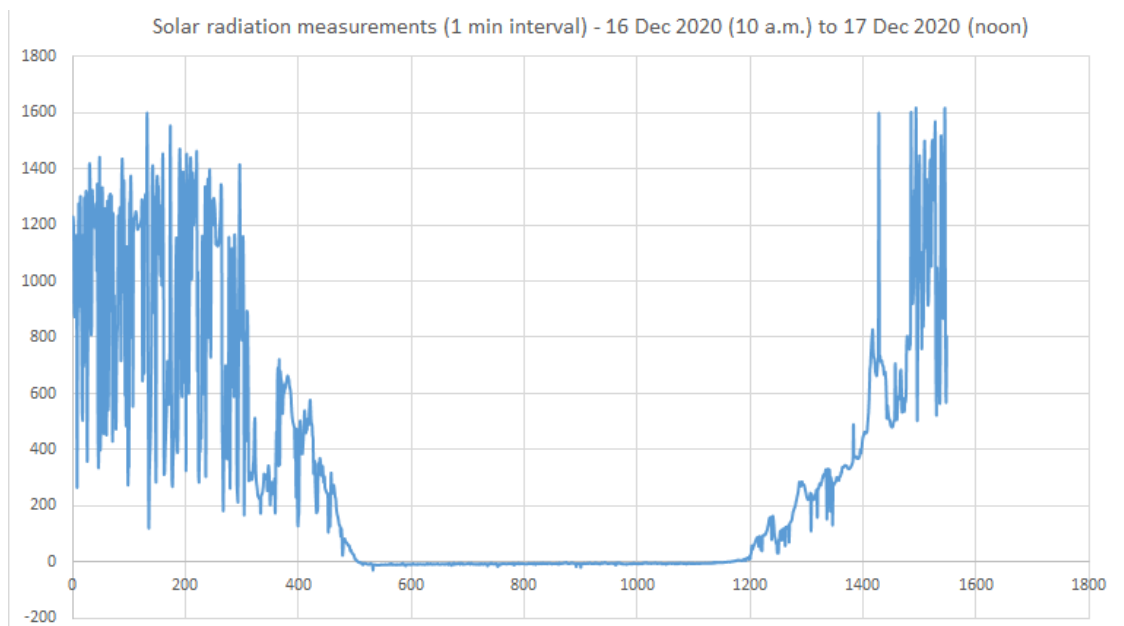


Figure 32: Period of high solar radiation

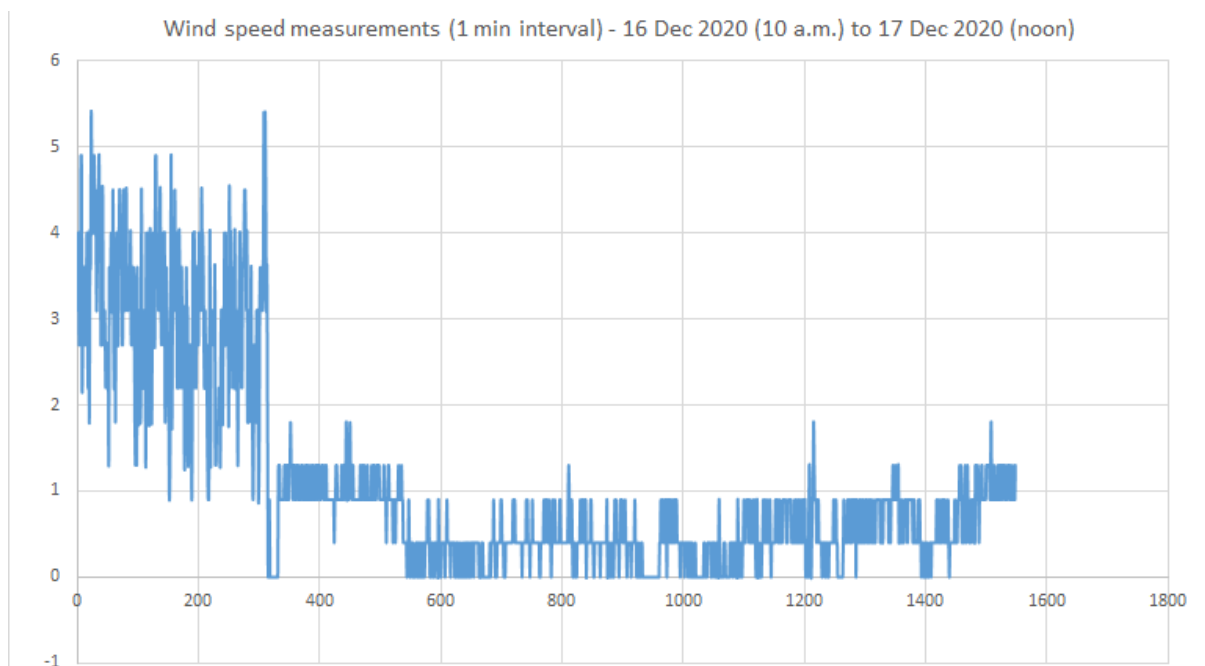


Figure 33: Wind speed measurements during selected period

As observed from Figure 33, the daytime period of 16 December 2020 had particularly high wind speeds up to 5 m/s, but the morning period of the following day was much calmer, making this period suitable to show the performance of the solar chimney in these situations. It is worth noting that the solar chimney as conceived in this project is to cater for passive ventilation in buildings in periods of no or low wind, and in the presence of wind, the wind pressure itself can be used to drive cross-ventilation through the interior spaces.

Due to the influence of external conditions on the measurements at location T4 (outlet), the temperature measurements at locations 2 and 3 are illustrated in Figure 34 against solar radiation on two separate axes. The increased temperatures at these two points with higher solar radiation are clearly observed.

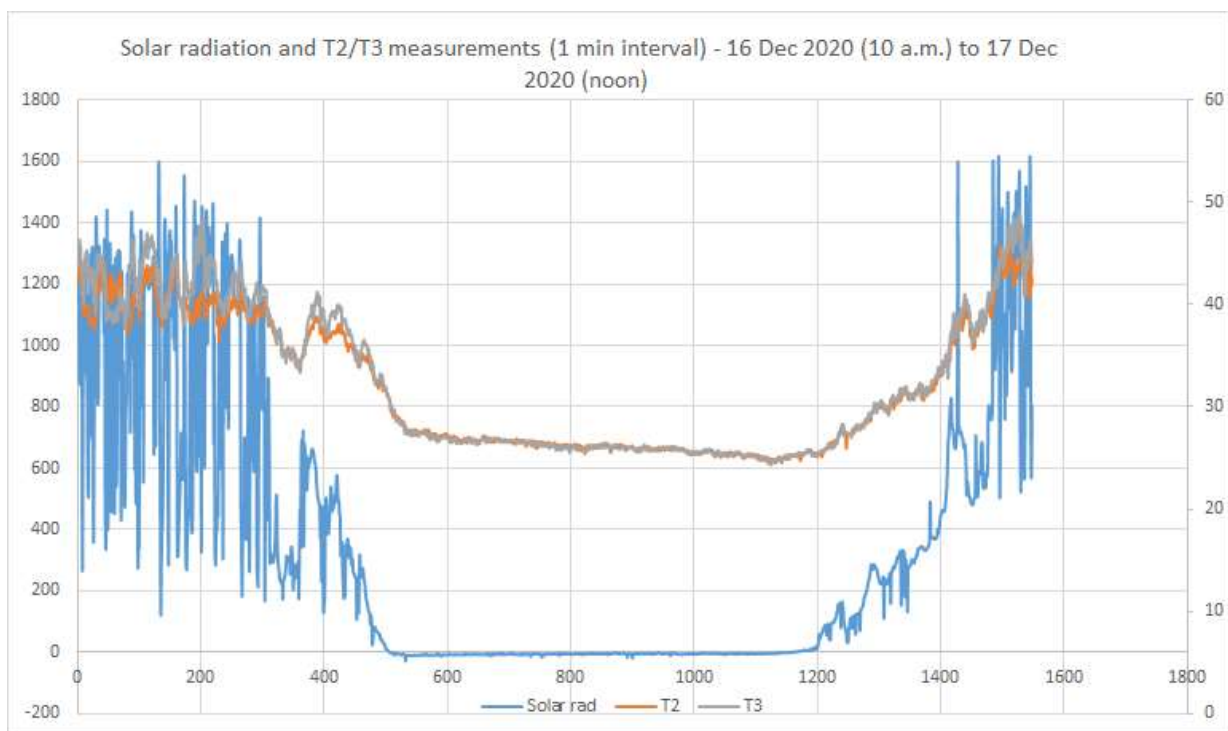


Figure 34: Variation of solar radiation with solar chimney internal temperature

Figure 35 illustrates the activity inside the solar chimney using the flow velocity at location 3 with respect to solar radiation. It is generally observed that with higher solar radiation, there is increased air flow inside the solar chimney. The other influencing parameter is the wind speed, which is depicted for the same period in Figure 36. As observed for the second day, with a much lower wind speed, there is still significant

activity inside the solar chimney, supporting the creation of the buoyancy effect when solar radiation is exposed on the system.

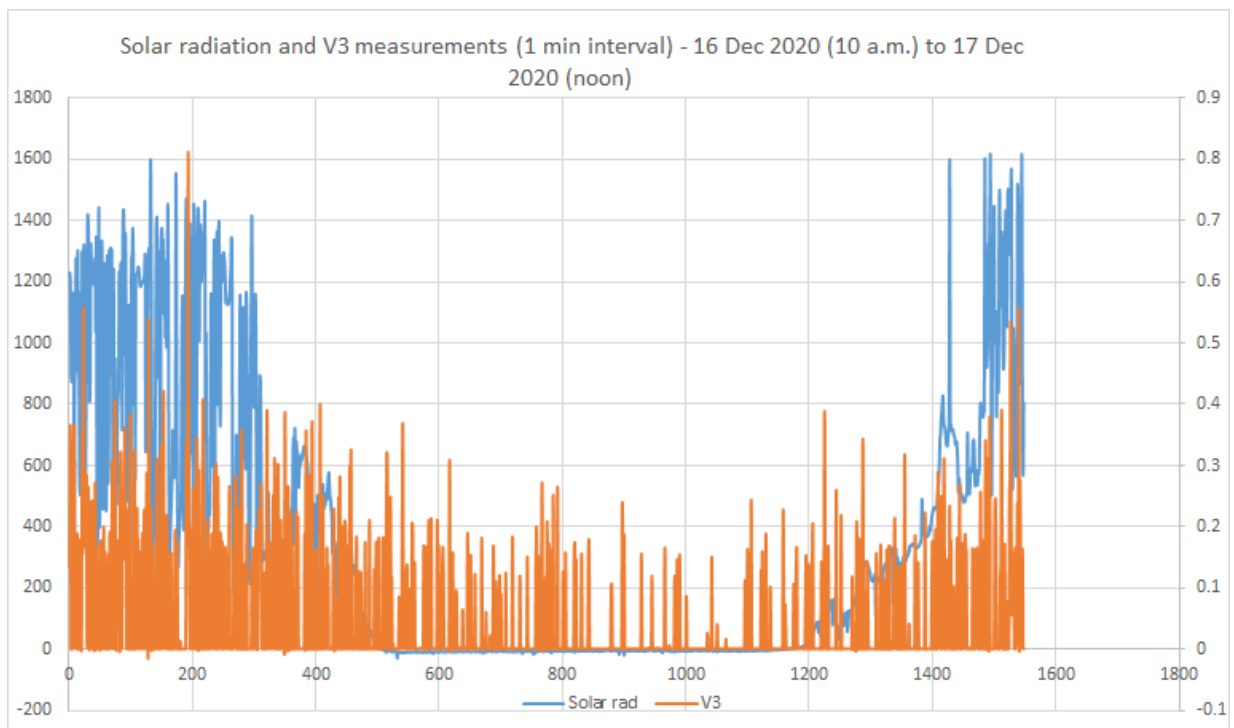


Figure 35: Variation of solar radiation with solar chimney internal flow

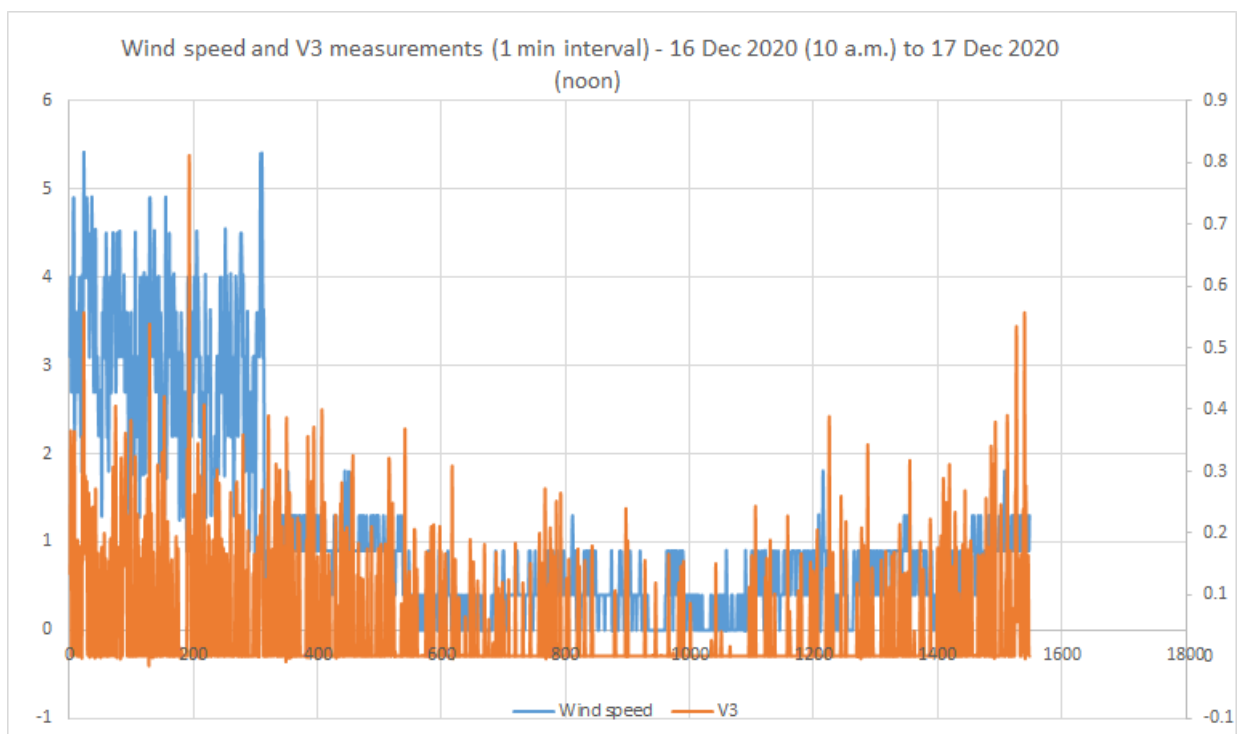


Figure 36: Variation of wind speed with solar chimney internal flow

6. Discussion and Conclusion

The flow and temperature values obtained via CFD simulations and experimentally show close agreement, with temperature between 30 and 45°C and flow velocities less than 1 m/s. Of prime importance for assessing the efficacy of natural ventilation systems is the air change rate per hour, which is estimated to be between 2 and 4 with the solar chimney system. Having validated the close agreement of the simulation and experimental values for the specific dimensions implemented, the results of the simulation can be extended for other dimensions modelled using CFD, and these results can be applied as design specifications to design solar chimneys for specific room dimensions. As hypothesized, the solar chimney system considered can be considered for both promoting cross-ventilation by expelling air from the interior space and also for supplying warm air to interior spaces, of specific interest for regions on the central plateau such as Curepipe and Vacoas where the beneficial warm air can be used to improve thermal comfort passively.

The proposed system can be installed either fixed to facades or roof mounted, as in both cases, the buoyancy force generated can be used to cause pressure gradient in interior spaces and lead to forced ventilation. The installation of a solar chimney on the roof is beneficial in being exposed to the sun throughout the day, hence promoting air flow for longer periods, whereas the façade mounted one will be exposed only during certain periods of the day, depending on orientation. However, roof-mounted system impose greater structural implications on the building, and may lead to water ingress problems during periods of heavy rainfall, which needs special attention.

The installation of several façade mounted system at strategic orientations can also be considered to achieve air flow for longer periods of time. The following illustrations (courtesy of Mr Giggs Bullia) depict the use of the proposed solar chimney design affixed to walls at ground level. The illustrations show the openings of the solar chimney to the outside in an arbitrary position to show the movement of the hot air moment up the cavity and to the outside better, although in practice and in the experimental set up used, the openings actually hinge from the top and the lower part opens, which would pose a lesser

problem with water ingress, although if the solar chimney is installed outside over permeable land, water ingress during rainfall should not pose an issue.

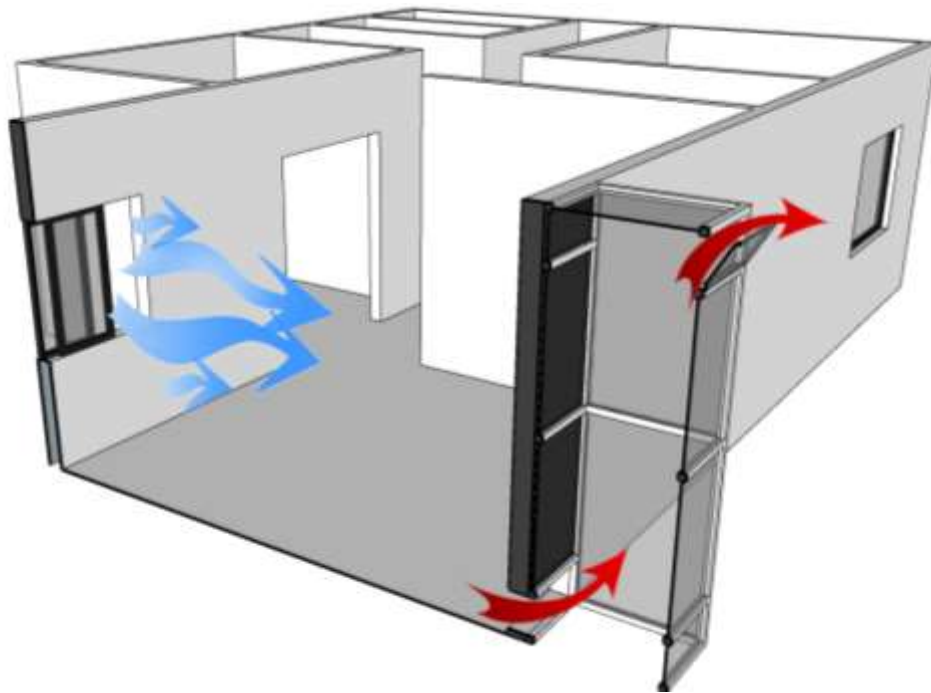


Figure 37: Illustrations of air movement through interior spaces and out of solar chimney (opening on solar chimney is shown hinging on the lower part to show the air movement out better, but in practice hinging at the upper part will be preferred as has been implemented in the experimental set up for the project)

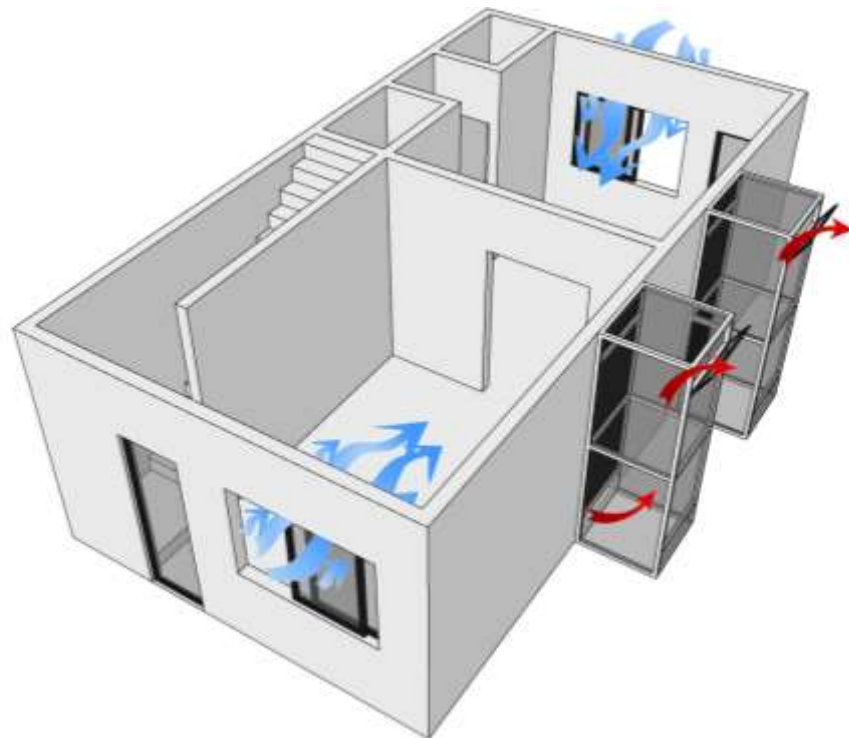


Figure 38: Combining multiple solar chimneys

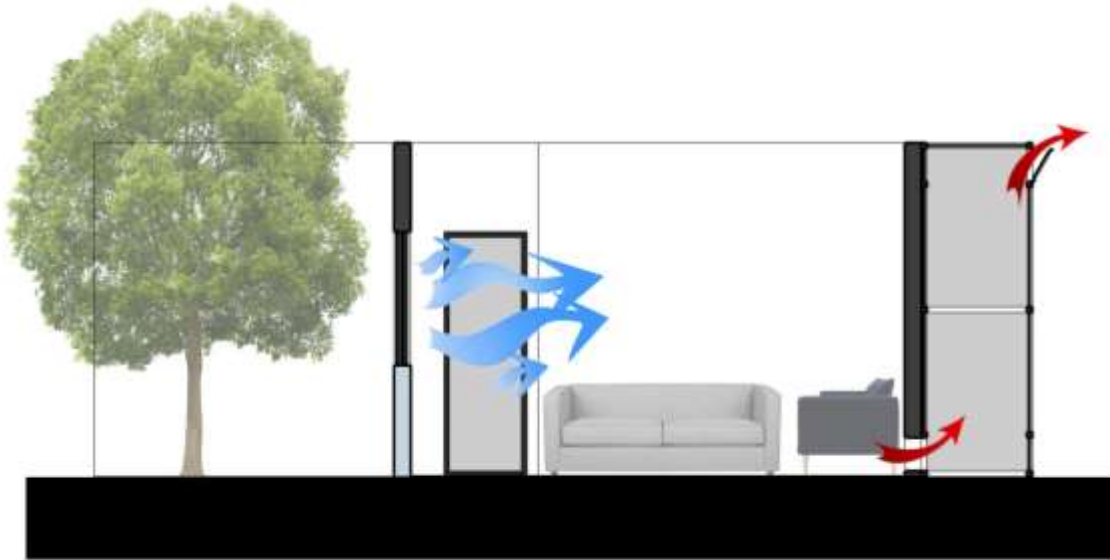


Figure 39: Use of solar chimney with landscaping to bring in fresh air from outside (openings are shown to hinge at lower level to better show air movement out of solar chimney, but in practice openings will hinge from the upper level)

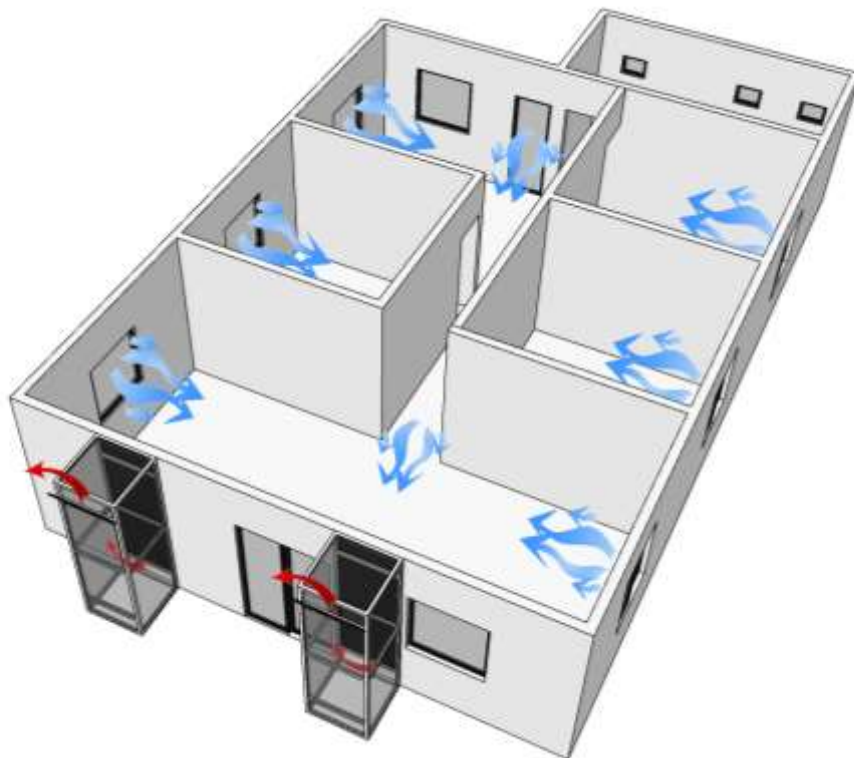


Figure 40: Driving air movement in a full layout by creating negative pressure using solar chimneys

In general, the research findings from the project has provided scientific data to support the use of solar chimneys in the local context, with good potential to improve thermal

comfort and air quality inside our buildings passively, and the proposed design can be integrated into the building structure so that sustainability is promoted without compromising on aesthetics. Furthermore, the proposed aluminium and glass pane design can be fabricated by local aluminium companies and is expected cost around Rs 15,000 per prototype. However, the concrete-based solar chimney with dark-coloured walls remains an option, albeit at much higher cost.

Bibliography

1. Abdeen, Ahmed & Bady, Mahmoud & Ookawara, Shinichi & Abdel-Rahman, Ali Kamel. (2016). Achieving standard natural ventilation rate of dwellings in a hot-arid climate using solar chimney. *Energy and Buildings*. 133. 10.1016/j.enbuild.2016.10.001.
2. Abdeen, A., Serageldin, A. A., Ibrahim, M. G., El-Zafarany, A., Ookawara, S. & Murata, R. (2019), 'Solar chimney optimization for enhancing thermal comfort in egypt: An experimental and numerical study', *Solar Energy* 180, 524–536.
3. AboulNaga MM, Abdrabboh SN. Improving night ventilation into low-rise buildings in hot-arid climates exploring a combined wall–roof solar chimney. *Renew Energy* 2000;19:47–54.
4. Abounaga, M.M, A roof solar chimney assisted by cooling cavity for natural ventilation in buildings in hot arid climates: an energy conservation approach in ALAIN city, *Renewable Energy* 14 (1998) 357–363.
5. Afonso, C. & Oliveira, A. (2000), 'Solar chimneys: simulation and experiment', *Energy and Buildings* 32(1), 71–79.
6. Aja, Ogboo & Al-Kayiem, Hussain & Abdul Karim, Zainal Ambri. (2013). Experimental investigation of the effect of wind speed and wind direction on a solar chimney power plant. *WIT Transactions on Ecology and the Environment*. 179. 945-955. 10.2495/SC130802.
7. Al Awadhi, A. & Hasan, M. (2011), *Comfort Assessment of a Fully/Semi-enclosed Courtyard: Case Study of Bahrain Low Rise Villa Housing Model*, PhD thesis, Citeseer.
8. Al-Kayiem, H. H., Sreejaya, K. & Gilani, S. I. U.-H. (2014), 'Mathematical analysis of the influence of the chimney height and collector area on the performance of a roof top solar chimney', *Energy and Buildings* 68, 305–311.
9. Andersen, K. T. (1995), *Theoretical considerations on natural ventilation by thermal buoyancy*, Technical report, American Society of Heating, Refrigerating and Air-Conditioning Engineers.
10. Anderson, J. D. & Wendt, J. (1995), *Computational fluid dynamics*, Vol. 206, Springer.

11. Asadi, Somayeh & Fakhari, Maryam & Fayaz, R. & Mahdavi Parsa, Mina. (2016). The effect of solar chimney layout on ventilation rate in buildings. *Energy and Buildings*. 123. 71-78. 10.1016/j.enbuild.2016.04.047.
12. Bouchair A. Solar chimney for promoting cooling ventilation in southern Algeria. *Building Services Engineering Research and Technology*. 1994;15(2):81-93. doi:10.1177/014362449401500203.
13. Buonomo, B., Manca, O., Montaniero, C. & Nardini, S. (2015), 'Numerical investigation of convective–radiative heat transfer in a building-integrated solar chimney', *Advances in Building Energy Research* 9(2), 253–266.
14. Capasso, L., Diana, A., Manca, O., Nardini, S. & Vigna, S. (2019), 'Numerical investigation on a solar chimney in a building facade under different climatic condition'
15. Charitar, D. (2015), Numerical study of the thermal performance of solar chimneys for ventilation in buildings, PhD thesis, University of Cape Town.
16. Charvat, P., Jicah, M. & Stetina, J. (2004), Solar chimneys for ventilation and passive cooling, in 'World Renewable Energy Congress, Denver, USA'.
17. Chung, L. P., Ahmad, M. H., Ossen, D. R. & Hamid, M. (2015), 'Effective solar chimney cross-section ventilation performance in malaysia terraced house', *Procedia-Social and Behavioral Sciences* 179, 276–289.
18. Chungloo, S. & Limmeechokchai, B. (2007), 'Application of passive cooling systems in the hot and humid climate: The case study of solar chimney and wetted roof in thailand', *Building and Environment* 42(9), 3341–3351.
19. Z. Chen, P. Bandopadhyay, J. Halldorsson, C. Byrjalsen, P. Heiselberg, Y. Li, An experimental investigation of a solar chimney model with uniform wall heat flux, *Building and Environment* 38 (2003) 893–906.
20. DeBlois, J. C. & Ndiaye, D. (2015), Cfd-assisted design and optimization of solar chimneys for elementary school classrooms, in '14th Conf. Int. Build. Perform. Simul. Assoc', pp. 818–825.
21. Ding WT, Hasemi Y, Yamada T. Natural ventilation performance of a double-skin façade with a solar chimney. *Energy Build* 2005;37:411–8.
22. Du W, Yang QR, Zhang JC. A study of the ventilation performance of a series of connected solar chimneys integrated with building. *Renew Energy* 2011;36:265–71.
23. El-Haroun, A. (2012), 'Performance evaluation of solar chimney power plants in egypt', *Inter- national journal of pure and applied sciences and technology* 13(2), 49. Energy, S. (2020), 'Knownlegde network'.
24. Gan, G. & Riffat, S. (1998), 'A numerical study of solar chimney for natural ventilation of buildings with heat recovery', *Applied Thermal Engineering* 18(12), 1171–1187.
25. Gan GH. A parametric study of Trombe walls for passive cooling of buildings. *Energy Build* 1998;27:37–43.

26. Godoy-Vaca, L., Almaguer, M., Martínez-Go´mez, J., Lobato, A. & Palme, M. (2017), Analysis of solar chimneys in different climate zones-case of social housing in Ecuador, in 'IOP Conference Series: Materials Science and Engineering', Vol. 245, IOP Publishing, p. 072045.
27. Gontikaki, M. & Trcka, Marija & Hensen, Jan & Hoes, Pieter-Jan. (2010). Optimization of a Solar Chimney Design to Enhance Natural Ventilation in a Multi-Storey Office Building. B. Ramadan, K. Nader, An analytical and numerical study of solar chimney use for room natural ventilation, *Energy and Buildings* 40 (2008) 865–873.
28. Harris, D. & Helwig, N. (2007), 'Solar chimney and building ventilation', *Applied Energy* 84(2), 135–146.
29. Hong, S., He, G., Ge, W., Wu, Q., Lv, D. & Li, Z. (2019), Annual energy performance simulation of solar chimney in a cold winter and hot summer climate, in 'Building Simulation', Vol. 12, Springer, pp. 847–856.
30. Khedari, Joseph & Rachapradit, Ninnart & Hirunlabh, Jongjit. (2003). Field study of performance of solar chimney with air-conditioned building. *Energy*. 28. 1099-1114. 10.1016/S0360-5442(03)00092-6.
31. Koronaki, I. (2013), 'The impact of configuration and orientation of solar thermosiphonic systems on night ventilation and fan energy savings', *Energy and buildings* 57, 119–131.
32. Lal, S. (2014), 'Cfd simulation for the feasibility study of a modified solar chimney applied for building space heating', *World Journal of Modelling and Simulation* 10(4), 293–307.
33. Lee, K. H. & Strand, R. K. (2009), 'Enhancement of natural ventilation in buildings using a thermal chimney', *Energy and Buildings* 41(6), 615–621.
34. Liping, W. & Angui, L. (2004), A numerical study of vertical solar chimney for enhancing stack ventilation in buildings, in 'The 21th Conference on Passive and Low Energy Architecture. Eindhoven, The Netherlands'.
35. Mathur, J., Bansal, N., Mathur, S., Jain, M. et al. (2006), 'Experimental investigations on solar chimney for room ventilation', *Solar Energy* 80(8), 927–935.
36. Mathur, J., Mathur, S. et al. (2006), 'Summer-performance of inclined roof solar chimney for natural ventilation', *Energy and Buildings* 38(10), 1156–1163.
37. Miyazaki, T., Akisawa, A. & Kashiwagi, T. (2006), 'The effects of solar chimneys on thermal load mitigation of office buildings under the Japanese climate', *Renewable Energy* 31(7), 987–1010.
38. Shahin Nasirivatan, Alibakhsh Kasaeian, Mehrdad Ghalamchi, Mehran Ghalamchi, Performance optimization of solar chimney power plant using electric/corona wind, *Journal of Electrostatics*, Volume 78, 2015, Pages 22-30, ISSN 0304-3886
39. K.S. Ong, A mathematical model of a solar chimney, *Renewable Energy* 28 (2003) 1047–1060.

40. Rahimi, M. & Arianmehr, I. (2011), 'The effect of a vertical vent on single-sided displacement ventilation', *ISRN Mechanical Engineering* 2011.
41. B. Ramadan, K. Nader, An analytical and numerical study of solar chimney use for room natural ventilation, *Energy and Buildings* 40 (2008) 865–873.
42. B. Ramadan & K. Nader. (2009). Effect of solar chimney inclination angle on space flow pattern and ventilation rate. *Energy and Buildings - ENERG BLDG.* 41. 190-196. 10.1016/j.enbuild.2008.08.009.
43. Waraporn Rattanongphisat, Piphat Imkong, Sutthinon Khunkong, An Experimental Investigation on the Square Steel Solar Chimney for Building Ventilation Application, *Energy Procedia*, Volume 138, 2017, Pages 1165-1170, ISSN 1876-6102.
44. Shi, Long & Zhang, Guomin & Yang, Wei & Huang, Dongmei & Cheng, Xudong & Setunge, Sujeeva, 2018, Determining the influencing factors on the performance of solar chimney in buildings," *Renewable and Sustainable Energy Reviews*, Elsevier, vol. 88(C), pages 223-238.
45. Sparrow, E. M. & Azevedo, L. (1985), 'Vertical-channel natural convection spanning between the fully-developed limit and the single-plate boundary-layer limit', *International Journal of Heat and Mass Transfer* 28(10), 1847–1857.
46. Spencer S. An experimental investigation of a solar chimney natural ventilation system. Canada: Concordia University; 2001.
47. C. Sudaporn, L. Budit, Application of passive cooling systems in the hot and humid climate: the case study of solar chimney and wetted roof in Thailand, *Building and Environment* 42 (2007) 3341–3351.
48. Sudprasert, S., Chinsorranant, C. & Rattanadecho, P. (2016), 'Numerical study of vertical solar chimneys with moist air in a hot and humid climate', *International Journal of Heat and Mass Transfer* 102, 645–656.
49. Wang, Y., Bakker, F., de Groot, R., Wortche, H. & Leemans, R. (2015), 'Effects of urban trees on local outdoor microclimate: synthesizing field measurements by numerical modelling', *Urban Ecosystems* 18(4), 1305–1331.
50. Wei, D., Qirong, Y. & Jincui, Z. (2011), 'A study of the ventilation performance of a series of connected solar chimneys integrated with building', *Renewable energy* 36(1), 265–271.
51. Zamora, B. & Kaiser, A. (2009), 'Optimum wall-to-wall spacing in solar chimney shaped channels in natural convection by numerical investigation', *Applied Thermal Engineering* 29(4), 762–769.
52. Zha, X., Zhang, J. & Qin, M. (2017), 'Experimental and numerical studies of solar chimney for ventilation in low energy buildings', *Procedia Engineering* 205, 1612.
53. Zhai, X., Dai, Y. & Wang, R. (2005), 'Experimental investigation on air heating and natural ventilation of a solar air collector ', *Energy and Buildings* 37(4), 373–381.

54. <https://www.instrumentchoice.com.au/instrument-choice/data-loggers/thermocouple-loggers/hobo-4-channel-thermocouple-data-logger-ux120-014m>
55. <https://knowledge.autodesk.com/company/sbd/buildings/trombe-wall-and-attached-sunspace>
56. <https://solarenergyengineering.asmedigitalcollection.asme.org>
57. <https://www.instrumentchoice.com.au/instrument-choice/data-loggers/thermocouple-loggers/hobo-4-channel-thermocouple-data-logger-ux120-014m>